NASA CR-72696

CIRCUIT EFFICIENCY ENHANCEMENT STUDIES AT 12 GHz

by

Dr. G. M. Branch

GENERAL ELECTRIC COMPANY

prepared for

NATIONAL AERONAUTICS AND SPACE ADMINISTRATION

NASA Lewis Research Center

Contract NAS3-11533

G. J. Chomos, Project Manager

Requests for copies of this report should be referred to

National Aeronautics and Space Administration
Scientific and Technical Information Facility
P.O. Box 33
College Park, Md. 20740

FINAL REPORT

CIRCUIT EFFICIENCY ENHANCEMENT STUDIES AT 12 GHz

by

Dr. G. M. Branch

GENERAL ELECTRIC COMPANY
Tube Department
Microwave Tube Operation
Schenectady, New York

prepared ~~by~~ for

NATIONAL AERONAUTICS AND SPACE ADMINISTRATION

May 29, 1970

CONTRACT NAS3-11533

NASA Lewis Research Center
Cleveland, Ohio
G. J. Chomos, Project Manager
Spacecraft Technology Division

FOREWORD

The work described herein was done by the General Electric Microwave Tube Operation under NASA Contract NAS3-11533 with Dr. G. M. Branch and Mr. R. E. Turrentine as principal investigators. Mr. G. J. Chomos, Spacecraft Technology Division, NASA-Lewis Research Center, was Project Manager.

TABLE OF CONTENTS

ABSTRACT

As part of a continuing program to develop the technology required for high-power broadcasting from satellite-borne television transmitters, an analytic and experimental study was conducted to enhance the efficiency of the system in utilizing available power by increasing the circuit efficiency of the klystron power amplifier. A new toroidal cavity was developed that effectively combines the high electron-beam interaction impedance capability of reentrant cavities with the lower internal power losses more characteristic of spherical cavities.

SUMMARY

A combined analytic and experimental study was carried out to develop methods for enhancing circuit efficiency in klystron power amplifiers intended for satellite-borne television broadcasting service. A new digital computer program employing a relaxation method for computing field distributions in microwave cavities was used extensively in the analysis of conventional cavity types and in the study of a new proposed toroidal cavity. The toroidal cavity was subsequently fabricated by coining and the experimentally observed properties of the cavity agreed closely with the analytically predicted properties.

The new toroidal cavity has a 40 percent higher internal Q than the internal Q of an equivalent conventional doubly-reentrant cavity with right-circular cylindrical outer wall and tunnel sections. Since the toroidal cavity can be readily constructed by die-forming, fabrication with high precision at high frequencies should be easier than with a conventional cavity.

In addition to developing the toroidal cavity parameters for a specific satellite-borne television transmitter application, methods of coupling the cavity to the output waveguide leading to the antenna were experimentally studied and a coupling means was devised.

INTRODUCTION

On May 27, 1969, a theoretical and experimental study was begun by the Microwave Tube Operation of the General Electric Company under NASA Contract NAS3-11533, with the objective of enhancing circuit efficiency in klystron power amplifiers to be used in satellite-borne television broadcast transmitters. Although the specific objective of the program was to advance the technology required to make satellite-borne television broadcasting more feasible, the methods developed for improved circuit efficiency would be advantageous in any microwave power system employing klystron power amplifiers. Improved efficiency in commercial land-based television transmitters, in radar systems and in high-energy particle accelerators can be achieved with the new type of klystron output cavity developed in this study.

In a previous study sponsored by NASA under Contract NAS3-11514,[1] the need for an improvement in circuit efficiency was recognized. Although this study demonstrated that additional transmitter efficiency in the utilization of available solar power could be achieved by the development of optimized klystron designs, only an improvement in design and fabrication of the cavity could reduce the power dissipated in the output circuit of the klystron. Accordingly, the present study was undertaken with the objective of exploring new cavity configurations and developing or evaluating methods of cavity fabrication that would lead to reduced ohmic power dissipation in the output cavity.

The specific application which served as a focus to make the study more objective and more directly applicable to presently foreseen developments was a satellite-borne television transmitter capable of broadcasting 4 kilowatts of CW power at a frequency of 12.2 GHz. Although two bandwidths were considered (40 MHz and 120 MHz), primary emphasis was placed on the 40-MHz bandwidth and the final cavity designs were developed for this bandwidth, only.

A recently developed computer program for the relaxation solution of field distributions in microwave cavities was used in the analytic phases of this study. This program was demonstrated to provide accurate computations of basic cavity parameters such as the impedance-bandwidth parameter R/Q and the product of the internal Q with the skin-depth-to-wavelength ratio parameter $Q\,\delta/\lambda$. This computer program was developed previously by the General Electric Company in association with an independent research effort.

An improved toroidal cavity with superior properties was developed in this study and is sketched in Figure 1. In the following sections the results of the analytic study, methods of fabrication, and testing of the toroidal cavity are described.

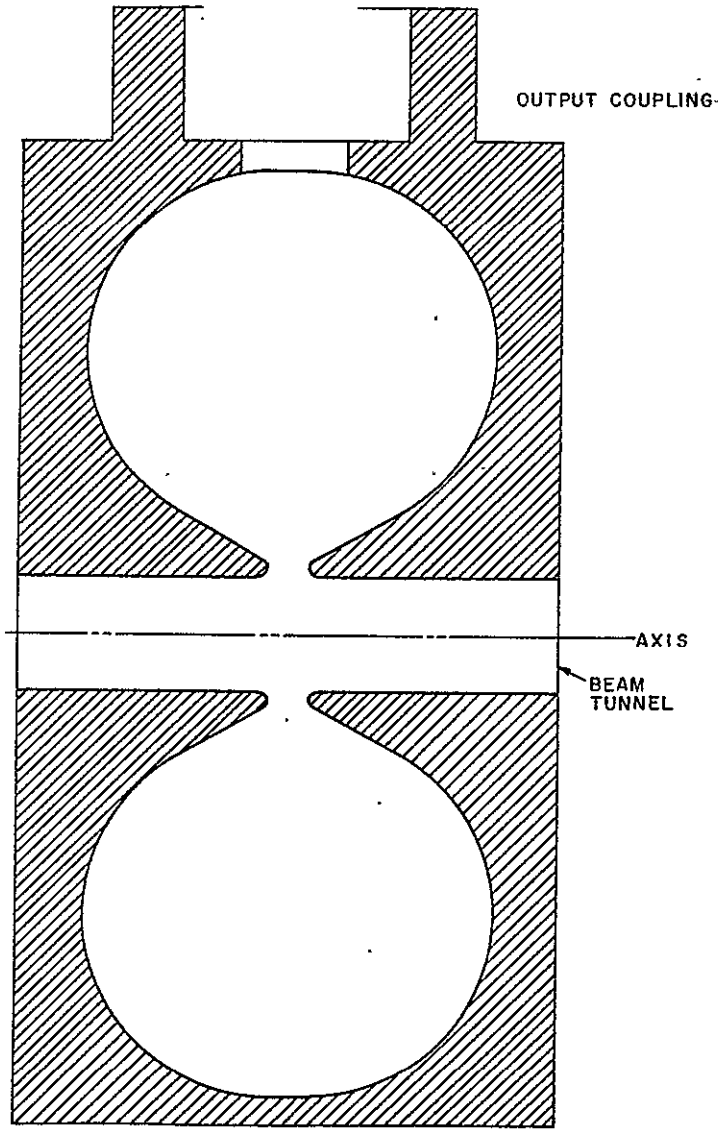

Figure 1 - Toroidal Cavity for Use as Output Interaction Circuit in Satellite-Borne TV Klystron

OPTIMIZATION OF CAVITY PARAMETERS BY ANALYTIC METHODS

COMPARISON OF CAVITY TYPES WITH INHERENTLY-LOW INTERNAL LOSSES

The basic cavity parameters relative to the electrical performance of a klystron are the cavity impedance-bandwidth parameter R/Q, the internal Q of the cavity Q_i (sometimes called the unloaded Q, Q_u), and the loaded Q, Q_ℓ. The parameter R/Q is the ratio of the shunt impedance of the beam interaction gap in the cavity of the loaded Q of the cavity. The parameter Q_i (or Q_u) is a measure of the internal power loss in the cavity due to surface currents flowing in the cavity. Q_ℓ, is a measure of the total power delivered by the beam to the cavity, which in turn dissipates a portion of the power by ohmic losses in the cavity and delivers the remainder through a port or iris to an output waveguide.

Another useful Q in relating to the power delivered to the external load by the cavity is Q_{ext}. From the definition of any of these Q's that

$$Q = \omega U/W \tag{1}$$

where ω is the 2π times the resonance frequency, U is the stored energy in the cavity, and W is the corresponding power load, it is seen that Q_{ext} is related to Q_ℓ and Q_i by

$$1/Q_{ext} = 1/Q_\ell - 1/Q_i \tag{2}$$

The circuit efficiency in terms of Q_ℓ and Q_i is given by

$$\eta_{ckt} = 1 - Q_\ell/Q_i \tag{3}$$

Consequently, the circuit efficiency may be enhanced by reducing Q_ℓ with an accompanying increase in the output circuit bandwidth, provided sufficient impedance R is retained to interact efficiently with the electron beam. Alternatively, the circuit efficiency may be enhanced by a cavity configuration that reduces the internal power losses so that Q_i is increased.

The parameter R/Q fundamentally relates only to the physical configuration of the cavity for a given mode of excitation; it is independent of scale

size, cavity resonance frequency or cavity surface resistivity. The impedance-bandwidth parameter is considered to be independent of the degree of cavity loading in the usual range of Q_ℓ values which have no distortion affect on the modal fields. By definition,

$$R/Q = V^2/2\omega U \tag{4}$$

Where V is the interaction gap peak rf voltage, ω is the angular resonance frequency and U is the total energy stored in the cavity. The voltage V is the integral of the rf field across the interaction gap at a given level of excitation in a specified (usually TM_{010}) mode:

$$V = \int_{gap} E(r,z)\, dz = E_m d \tag{5}$$

Here E_m is an effective field amplitude, the product of which with the tunnel tip to tip distance d yields the gap voltage. The amplitude E_m may be used also to normalize the integral of the energy U stored at resonance in the cavity:

$$U = 1/2\, \epsilon \int_{vol} E^2(r,z)\, d\tau = 1/2\, \epsilon\, E_m{}^2\, g\, \bar{a}\, d^2 \tag{6}$$

where g is a field configuration integral independent of cavity scaling, resonance frequency or level of excitation. In this expression the cavity volume has been factored out and expressed as the product of the square of the gap length times a scaling length $\bar{a}$. From a combination of equations (5) and (6) with (4), the impedance-bandwidth parameter R/Q is given by

$$R/Q = \eta/k\bar{a}g \tag{7}$$

where k is the propagation constant ω/c or $\omega/\sqrt{\mu\epsilon}$ and η is the intrinsic impedance of free space $\sqrt{\mu/\epsilon}$, which is approximately 120π ohms. Since the resonance frequency varies inversely with the scaling of the cavity, the quantity $k\bar{a}$ is a constant for a given resonance mode and hence R/Q is invariant with scaling.

Another basic cavity parameter that is a function only of cavity configuration and type of mode is the quantity $Q\delta/\lambda$, where Q is the cavity internal Q, δ is the skin depth of the metal composing the cavity walls and λ is the free space wavelength corresponding to the resonance frequency.

In terms of the surface resistivity R_s, the ratio δ/λ is given by:[2]

$$\delta/\lambda = R_s/\pi\eta \tag{8}$$

From equations (1) and (8), the product $Q\,\delta/\lambda$ is therefore given by:

$$Q\,\delta/\lambda = \omega U R_s/\pi\eta W_i \tag{9}$$

As before, U may be expressed as a volume integral, this time of the square of the magnetic field, and the volume is again factored out and expressed in terms of a scale dimension $\bar{a}$, the product of which with the surface area A yields the volume:

$$U = 1/2\,\mu \int_{vol} H^2(r/z)\,d\tau = 1/2\,\mu\,\overline{H_v^2}\,\bar{a}\,A \tag{10}$$

where $\overline{H_v^2}$ is the mean square of the magnetic field over the volume of the cavity. Similarly, in terms of the mean square of the magnetic field H over the surface of the cavity (corresponding to the mean square of the surface current density J over the surface of the cavity), the ohmic power loss W_i may be written as:

$$W_i = 1/2\,R_s \int_{surface} H^2(r,z)\,dS = 1/2\,R_s\,\overline{H_s^2}\,A \tag{11}$$

Finally, from (10) and (11),

$$Q\,\delta/\lambda = \pi k\bar{a}\,\overline{H_v^2}/\overline{H_s^2} \tag{12}$$

This parameter is thus independent of frequency or surface resistivity since the ratio of the two magnetic field mean squares is a function of mode configuration only.

In order to assess the available magnitudes of the parameters R/Q and $Q\,\delta/\lambda$, the theoretical properties of cavities of simple physical configurations (cylinders or spheres) may be considered. In addition, one should examine the computed or measured properties of doubly-reentrant cavities of the type required for efficient interaction with an electron beam

in a klystron. The theoretical expressions for R/Q and $Q\delta/\lambda$ for a rectangular parallelopiped of length d, height a and width a, for a right circular cylinder of length d and radius a, and for a sphere of radius a are given in Table I. A reasonable basis for comparison of the above three types is to specify that they have equal volumes and also resonate at the same frequency. Each cavity is assumed to resonate in its lowest fundamental mode with uniform electric fields parallel to the direction of the dimension d; ie, the modes to be considered are the TM_{110}, the TM_{010}, and the TM_{101} for the rectangular, cylindrical and spherical cavities, respectively. (In the spherical cavity the interaction gap length d is equal to 2a.) The theoretical values of R/Q, $Q\delta/\lambda$, ka, and d/a at the same resonance frequency and same cavity volume are given in Table II.

It will be noted in Table II that the values of R/Q and the interaction gap lengths are not appreciably different for the three cavity types. The spherical cavity has the highest value of $Q\delta/\lambda$ and hence the lowest internal loss with the cylindrical cavity ranking next.

It would appear that in order to reduce the internal losses, the number of right angle bends and corners must be reduced as much as possible.

The above three basic shapes are not of practical use for cavities employed in interacting with electron beams because of the long transit angle that the beam electrons would experience in traversing the interaction gap of length d. Even at a highly relativistic electron velocity approaching c, the transit angle would be about 5 radians in such cavities, whereas a value of about 1 radian or less is required for good interaction. The transit-time dependent beam coupling coefficient in interaction gaps with axial electric fields of uniform magnitude is given by the ratio $\sin\theta/\theta$, where θ is the half-transit angle,[3] so that with transit angles of less than 1 radian the coupling coefficient will be higher than 0.8415.

Improved coupling is obtained in cavities designed for use in klystrons by introducing a reentrant tunnel or a pair of opposing tunnels to reduce the interaction gap length. In a singly-reentrant cavity, the interaction gap is defined as the region between the end of the tunnel and the opposing flat cavity wall, whereas in doubly-reentrant cavities the gap is located between the two ends of the opposing tunnels. The tunnels as well as the wall in the singly-reentrant cavity contain apertures for the passage of the electron beam. The introduction of the reentrant portions into the cavity provides additional internal conducting surfaces and corners which increase the internal ohmic loss; this compromise is necessary, however, in order to achieve a useful impedance level in the interaction gap.

TABLE I - R/Q and $Q\delta/\lambda$ FORMULAS FOR BASIC CAVITIES

Cavity Type	R/Q	$Q\delta/\lambda$
Rectangular	$\left[\eta\,(d/a)\right]/ka$	$\left[d/(d+a)\right]/2\sqrt{2}$
Cylindrical	$\left[\eta(d/a)\right]/ka/\left[\pi\ J_1^{\,2}\,(ka)\right]$	$\left[d/(d+a)\right]/\left[2\pi/ka\right]$
Spherical	$\left[\eta(d/a)\right]/ka/\left[\pi\ F_1(ka)/F_2(ka)\right]$ *	$\left[d/(d+a)\right]/\left[2\pi/(3ka/2 - 3/ka)\right]$

$$^{*}\ F_1(ka) = 2\left[(ka\cos ka)^2 - \sin^2 ka\right]$$

$$F_2(ka) = 3\left[\cos ka - (\sin ka)/ka - \sum_{n=1}^{\infty} \frac{(-1)^n\ ka^{2n}}{(2n-1)\ (2n-1)\ !}\right]^2$$

- - - - - - - - - - - - - - - -

TABLE II - THEORETICAL PROPERTIES OF FUNDAMENTAL MODES IN BASIC CAVITIES

Cavity Type	Mode	ka	d/a	R/Q	$Q\delta/\lambda$
Rectangular	TM_{110}	2.22144	1.9731	334.6	0.23463
Cylindrical	TM_{010}	2.40483	1.9802	366.4	0.25431
Spherical	TM_{101}	2.74371	2.0000	326.4	0.32066

- - - - - - - - - - - - - - - -

In general, because higher impedance is achievable in a doubly-reentrant cavity it is preferable to a singly-reentrant cavity. The R/Q of the singly-reentrant cavity suffers because the flat wall opposing the end of the reentrant tunnel generates an excessive shunt capacitance that reduces the gap impedance.

Multiple interaction gaps may be employed to provide extended interaction between an electron beam and a resonating circuit. Although higher effective impedances can be developed from properly cascaded and coupled interaction gaps, the internal Q of such a resonator may be expected to be inherently low. This is because of the increased amount of conductive surfaces of the septa that must be introduced into the resonator to support the

internal drift tunnels and to establish the boundary conditions for the desired spatial mode. In extremely broadband circuits having bandwidths approaching those of traveling wave tubes, the loaded Q, Q_ℓ, become effectively so low that the circuit efficiency as given by equation (3) reaches a tolerable level in spite of the relatively low value of Q_i characteristic of extended interaction circuits. At the relatively narrow bandwidths specified in the present study, the adopted approach in the search for higher circuit efficiency is to leave Q_ℓ fixed near its specified value and search for new types of single-gap cavities with higher internal Q's than are now achieved in conventional doubly-reentrant cylindrical cavities.

A typical doubly-reentrant cylindrical cavity is characterized by an R/Q in the range of from 100 to 150 ohms and a $Q\,\delta/\lambda$ value of between 0.04 and 0.1. Specific values that are considered to be achievable in conventional cavities for the klystrons intended for television broadcasting at 12.2 GHz in satellite-borne transmitters are discussed in the following section.

PARAMETRIC ANALYSIS OF OPTIMUM KLYSTRON DESIGNS

Before optimization studies for maximum circuit efficiency can be carried out, the basic cavity requirements for the 12.2 GHz klystron power amplifier capable of transmitting 4 kilowatts must be established. A parametric analysis based on an accurate simulation of the complete klystron is required because trade-offs between factors leading to broad bandwidth and those leading to maximum conversion efficiency must be evaluated. The basic parameters that will constrain the output cavity design will include the beam voltage, the minimum limit on the output cavity R/Q, the tunnel diameter, and the anticipated unavoidable beam interception. Additional constraints will be that the proposed cavity designs must be compatible with the space environment and hence must be rugged, dimensionally stable, and amenable to heat-pipe temperature control or other methods of cooling by conduction or convection.

Using design principles described in a prior study of high-efficiency klystrons for satellite-borne television transmitters,[1] a series of computations of conversion efficiency and bandwidth of 12.2 GHz klystrons at the 4-kilowatt power level was carried out on a high-speed digital computer, with beam perveance and output gap transit angle as the independent parameters. The beam microperveance was varied in steps of 0.5 from 0.5 to 2.0, and the output gap transit angle was varied from 0.5 to 2.0 radians in steps of 0.5 radian. For these computations, the normalized tunnel radius

was maintained at a constant value of $\gamma a = 1.0$, and the beam filling factor was maintained at $b/a = 0.6$. In the above mentioned study these parameters were shown to be feasible and to lead to high efficiency. The required beam power and hence the required beam voltage was determined from the computed efficiency.

Preceding the computation of efficiency at each perveance and gap transit angle, values of R/Q and Q_u for a conventional cylindrical doubly-reentrant output cavity with beveled tunnel tips were determined from a series of computations of these parameters as a function of tunnel wall thickness. The following semi-empirical analytic formulas as previously developed were used:[4]

$$R/Q = 120\ d/a\,(0.461/\sqrt{d/a} + 0.762\ ka - 0.244)(1 - 0.36\ ka)/ka \qquad (13)$$

$$Q_u = 4.09\ d/a \times 10^{10}/(\sqrt{f} \times R/Q) \qquad (14)$$

where d is the interaction gap length, a the tunnel outer radius, and k the frequency constant ω/c.

The cavity impedance parameter R/Q decreases because of the increased shunt capacitance generated by increased tunnel wall thickness. Also, the tunnel thermal conductance increases as the tunnel wall thickens. Therefore, the minimum wall thickness consistent with the maximum tolerable tunnel tip temperature should be chosen for maximum cavity impedance, maximum efficiency and bandwidth. As in the previous study,[5] a temperature drop of approximately 250°C is considered to be admissible since the heat-pipe cooling of the wall with a fluid temperature of 150°C prevents the tunnel tip from exceeding a safe operating temperature of 400°C.

The trend of the temperature differential, loaded Q and circuit efficiency with increasing tunnel wall thickness for a typical case is illustrated in Figure 2. Since the cavity impedance parameter R/Q decreases with increasing wall thickness, the value of Q required to yield the optimum beam interaction impedance rises with a consequent reduction in bandwidth. In the case illustrated, a tunnel with an outer diameter of approximately 0.118 inch and an inner diameter of 0.064 inch is required in order to provide maximum impedance and bandwidth for an allowable temperature differential of about 250°C. The beam power interception on one tunnel tip is assumed to be 58 watts, or 1 percent of the total beam power.

From a large number of large-signal disk model computations of klystron performance as a function of beam perveance and gap transit angle,

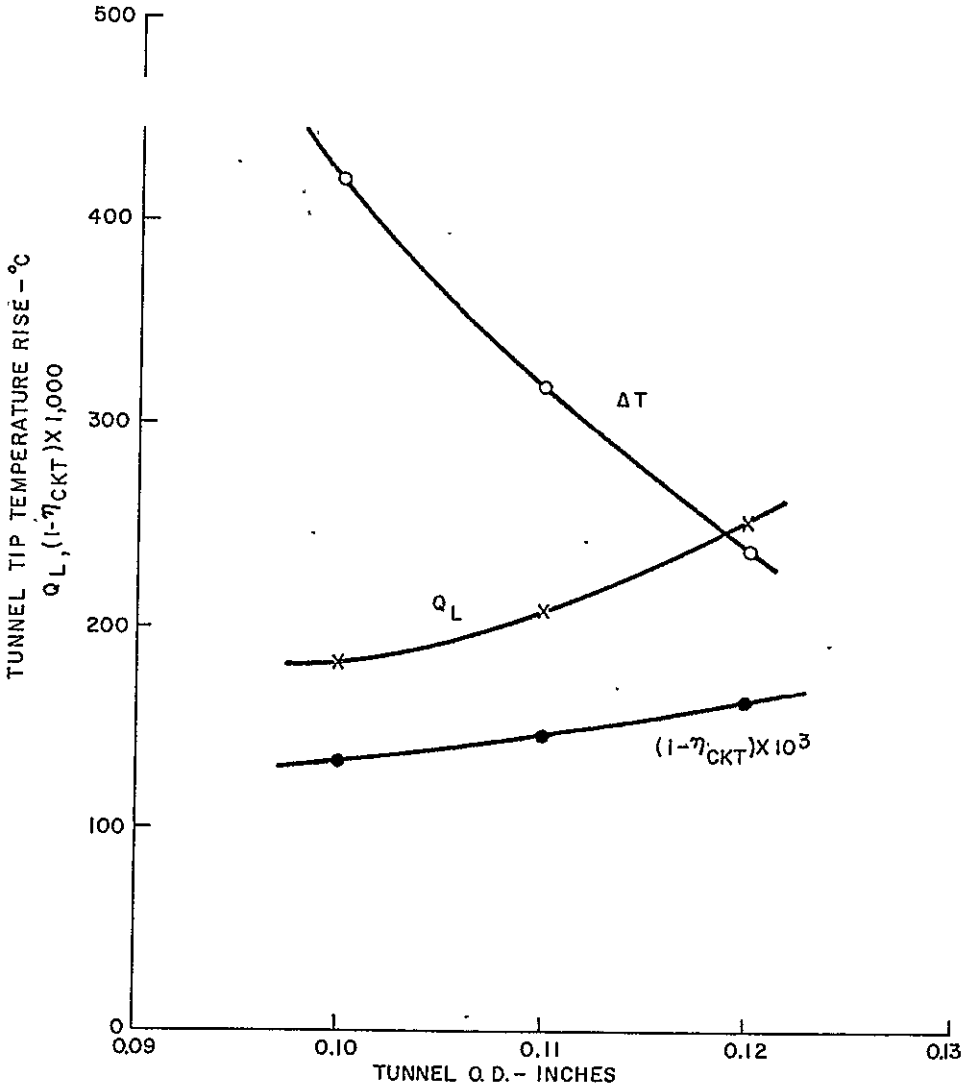

Figure 2 - Computed Variation of Tunnel Tip Temperature Differential, Minimum Permissible Value of Q_ℓ, and Corresponding Circuit Efficiency as Function of Tunnel Outer Diameter (Fixed Tunnel Inner Diameter)

the relationship between available bandwidths and the expected maximum available klystron power conversion efficiency was developed and is presented in graphical form in Figure 3. The computed klystron performance pertains to the type of klystrons designed in the previous study for satellite-borne television transmitters.[1] Increased efficiencies are achievable only at the lower bandwidths and the trade-off of efficiency for higher bandwidths is clearly seen.

Klystron power amplifiers with bandwidths of either 40 MHz or 120 MHz, corresponding to percentage bandwidths of 0.33 and 1.0 percent, were considered in the present study. The optimum choices for the beam microperveance and output gap transit angle, as shown in Figure 3, are 0.5 microampere/volt$^{1.5}$ and approximately 0.8 radian, respectively. For the 1.0 percent bandwidth klystron, a beam microperveance of 1.0 microampere/volt$^{1.5}$ and a gap transit angle of about 0.8 radian should be specified.

Tentative specifications for klystrons providing the required bandwidths of 40 and 120 MHz and capable of providing a continuous output of 4 kilowatts with optimum efficiency are listed in Table III.

The cavity dimensions shown in Table III correspond to those computed for conventional doubly-reentrant cylindrical cavities with beveled tunnel tips. One of the principal objectives of the present study is to develop a new cavity configuration having the values of Q_u inherently higher than 1790 and 1640 as predicted for the conventional cavities shown in the table.

METHODS OF CAVITY ANALYSIS

A new method of solving Maxwell's equations by successive over-relaxation, has been the principal analytic procedure used in this search for methods of improving circuit efficiency in satellite-borne klystron power amplifiers. In the case of transverse magnetic modes in resonators having axial symmetry, the wave equation for the magnetic field H (only a circumferential component exists) reduces to a Helmholtz equation that can be expressed in finite difference form. In a computer programming procedure -- similar to that previously used for solving Poisson's equation for electrostatic fields -- a variably-spaced mesh of lines normal to the z axis and of lines normal to the radius in a plane passing through the axis is laid over the boundaries of the axially symmetric cavity. An iterative computation is then employed so the H field at every mesh node will be properly related by the difference equations to the H field at adjacent nodes. This is subject to the constraint that the boundary conditions on the electric field be satisfied

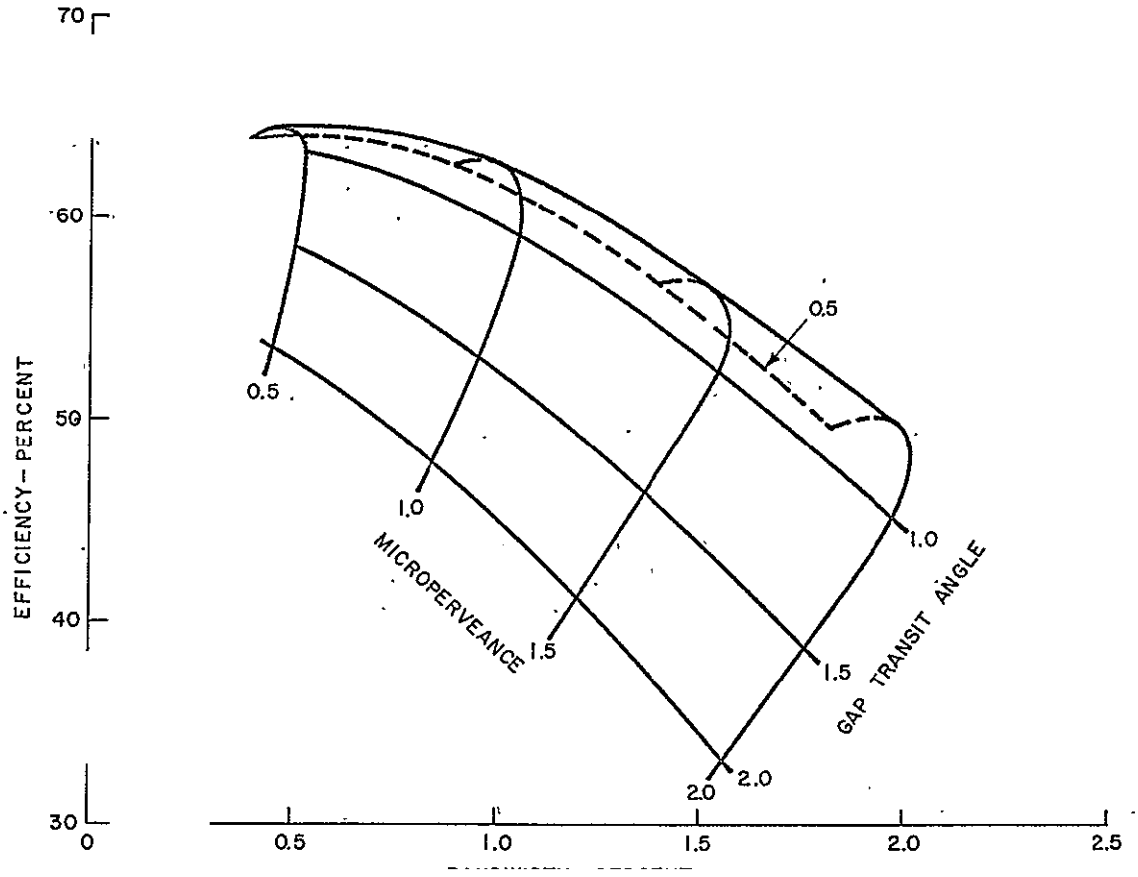

Figure 3 - Constant Perveance and Constant Gap Transit Angle Contours on Efficiency-Bandwidth Surface as Computed for Satellite-Borne TV Klystrons

TABLE III - TENTATIVE 12.2-GHz KLYSTRON DESIGN PARAMETERS

	Narrowband	Broadband
Bandwidth (nominal)	40 MHz	120 MHz
Bandwidth (3 dB)	52 MHz	121 MHz
Center frequency	12.2 GHz	12.2 GHz
Power output	4.0 kW	4.0 kW
Beam power	6.35 kW	6.68 kW
Beam voltage	11.0 kV	8.5 kV
Beam current	0.577 ampere	0.785 ampere
Overall conversion efficiency	63.4 percent	60.0 percent
Circuit efficiency	87.1 percent	95.4 percent
Cavity R/Q	83 ohms	102 ohms
Output gap transit angle	0.76 radian	0.81 radian
Output tunnel tip temp. rise	264 ^{o}C	259 ^{o}C
Output cavity Q_u	1790	1640
Output cavity Q_ℓ	230	101
Tunnel I.D.	0.066 inch	0.0574 inch
Tunnel I.D.	0.168 cm	0.146 cm
Tunnel O.D.	0.120 inch	0.100 inch
Tunnel O.D.	0.305 cm	0.254 cm
Output gap length	0.024 inch	0.0226 inch
Output gap length	0.061 cm	0.0574 cm

- - - - - - -

at all dielectric or metallic interfaces and boundaries. Satisfaction of the boundary conditions at nodes on or near the boundaries is achieved through the definition of 45 sets of influence coefficients for each of the types of normal or inclined intersections that may occur between a mesh line and a conducting or dielectric boundary. None of the cavities studied during this program contained a dielectric interface in the cavity.

A high-speed digital computer is used to index through the mesh consisting up to 100 horizontal (z) lines, 100 vertical (r) lines and with a maximum of 10,000 nodes. The number of nodes usually required to express adequately the boundary conditions is approximately 3000. The number of sweeps through the mesh required to reduce the residual error in the H field solution to less than 1 part in 10^6 is usually less than 300 with normal boundaries; however, the required number may reach 700 or 800 for cavities containing many mesh line intersections with inclined surfaces.

After a field solution for the H field is achieved for an estimated resonance frequency, the magnitudes of the radial and electric fields are computed at each node from the derivatives of the H field as defined by the curl equations Subsequently, the energy stored in both the magnetic field and the electric fields are computed over the volume of the cavity. If the two volume integrals of energy fail to agree, as they are required to do at resonance, the frequency is adjusted and the entire computation is repeated.

In the program, the gap voltage is obtained by an integration of the axial component of the computed electric field across the integration gap. From the volume integral of the stored energy and the surface integral of the square of the surface current density, the parameters R/Q and $Q\,\delta/\lambda$ are computed according to the formulas given in equations (4) and (12) above.

The accuracy of the program was tested by computing by relaxation the resonance frequency, R/Q and $Q\,\delta/\lambda$ for cavities in which these parameters were exactly known theoretically or for other cavities in which these parameters were experimentally measured.

Since the present computer program is restricted to the analysis of axially symmetric cavities, only the cylindrical and the spherical cavities of the three basic types considered above, can be analyzed. For this comparison, the right circular cylindrical cavity is assumed to have a height d equal to its radius a. The theoretical and the computed values of the cavity parameters are shown in Table IV.

For the computations given in Table IV, the theoretical value of ka was used initially and the energy balance indicating resonance was demonstrated to 1 part in 10^4 and to 1 part in 10^3 for the cylindrical and spherical cavities, respectively. Faster convergence and more accurate results were obtained in the case of the simple cylindrical cavity, but as indicated by the results in Table IV, the accuracy obtained in the analysis of the spherical cavity was satisfactory.

TABLE IV - COMPUTED AND THEORETICAL PARAMETERS OF BASIC CAVITIES

Cavity Type	ka		R/Q (ohms)		$Q\delta/\lambda$	
	Comp.	Theo.	Comp.	Theo.	Comp.	Theo.
Cylindrical	2.4048	2.4048	185.2	185.2	0.1913	0.1914
Spherical	2.7437	2.7437	308.0	326.4	0.3143	0.3206

- - - - - - -

A comparison of the computed and the experimentally measured parameters for three typical doubly-reentrant cavities with cylindrical tunnels and beveled tunnel tips is given in Table V. The cavity designated "NASA Cavity C" is a demountable cavity used in the previous study to provide an empirical calibration of the R/Q formula given in equation (13).[4]

- - - - - - - -

TABLE V - COMPUTED AND MEASURED PARAMETERS OF DOUBLY-REENTRANT CAVITIES

Cavity Type	ka		R/Q (ohms)		$Q\delta/\lambda$
	Comp.	Meas.	Comp.	Meas.	Comp.
L-Band	1.282	1.277	134	124	0.0800
S-Band	1.61	1.61	112	106	0.0995
NASA Cavity C	0.64	0.65	155	143	0.0469

- - - - - - - -

For the above cavities, all of which were demountable, the parameter $Q\delta/\lambda$ was not measured. Although good agreement is noted between the computed and observed resonance frequencies, in all cases the computed value of R/Q is a few percent higher than the measured quantity. It is not known whether the discrepancy is due to a systematic error in the computation or in the measurement.

TOROIDAL CAVITY DESIGN DEVELOPMENT

As seen in Table II, the parameter $Q\,\delta/\lambda$ is higher in a spherical cavity than in the right circular cylindrical cavity from which conventional doubly-reentrant cavities are developed. Consequently, it is reasonable to expect that an analogous development of doubly-reentrant cavities originating from a spherical cavity should provide good interaction impedances combined with some of the low-loss characteristics of the spherical cavity.

A sphere modified by a pair of reentrant conical tunnels becomes toroidal in shape. A toroidal cavity thus consists of a torus defining the outermost boundaries of the cavity and a pair of truncated cones, which are tangent at their circle of intersection with the torus and define the inner surface and the interaction gap.

Although toroidal cavities have found little practical application in the history of the development of klystrons, it is interesting to note that one of the earliest klystrons ever reported employed toroidal cavities.[6] These cavities consisted of a torus in which the inner surface was cut by a pair of grid planes perpendicular to the torus axis, the grid planes defining the interaction gap. Two decades later, Chodorow, Ginzton, Jasberg, Lebacqz and Shaw reported an X-band klystron that contained cavities similar to toroids in shape. The cavity shape consisted of a flattened sphere with right-circular cylindrical reentrant tunnels entering the two flat faces.[7]

There are many possible variations in the configuration of a toroidal cavity with reentrant tunnels. In order to describe such cavities in a systematic way it is necessary to develop a standard set of parameters. Assuming that abrupt changes in direction of the inner walls of the cavity will lead to local field concentrations with a consequent increase in internal cavity losses, only toroidal cavities generated by curved and straight line sections with tangent intersections will be assessed. With this restriction in mind, the toroidal cavities to be described can be considered to be generated by a curve composed in general of straight and curved tangent line segments rotated about a central axis.

The generating curve originates with a straight line segment which forms the outer surface of the cavity and is also tangent to an arc (the toroidal arc) which forms the principal rounded portion of the toroidal cavity. The opposite end of this arc is tangent to an inclinded straight-line segment which generates the outer wall of the conical reentrant tunnel. Further, the inclined straight-line segment is tangent to the arc that forms the tunnel

tip. Finally, the arc of the tunnel tip is tangent to the straight line segment which is parallel to the axis and generates the inner wall of the beam drift tunnel. The cross-section of one-half of a bisymmetric toroidal cavity with conical reentrant tunnels is illustrated in Figure 4.

The definition of the parameters describing the standard toroidal cavity are as follows:

w	=	width of the flat portion of the outer wall
r_a	=	radius of toroidal arc
θ	=	inclination angle of conical tunnel wall
r_t	=	radius of curvature of tunnel tip
a_i	=	inner radius of reentrant tunnel
d	=	interaction gap length between tunnel tips.

The above parameters form an independent set and are sufficient to prescribe the complete configuration of the standard toroidal cavity with conical reentrant tunnels in which all straight and curved surfaces form only tangent intersections.

By beginning at some reference point (e.g., on the axis at the interaction gap midplane), one can proceed to build up a table of coordinate pairs for each line segment interaction in order to specify the boundaries for the relaxation solution of the electromagnetic fields in the cavity. A short time-sharing digital computer program for generating the coordinate table from the above list of parameters was written and is included in Appendix A.

As a result of the above optimization studies related to the objective frequency, power level, and bandwidth, the following parameters were held constant for a comparison of the properties of cavities that could be employed in the specified klystrons:

d	=	0.020 inch
θ	=	20 degrees
a_i	=	0.030 inch
r_t	=	0.005 inch

Relaxation solutions of the electromagnetic fields were implemented for a series of cavity resonators to provide a reference from which improvement in internal Q for new cavity types could be measured. Both conventional doubly-reentrant cavities with rounded or beveled tips and toroidal cavities were investigated. The beam tunnel diameter of 0.060 inch and the

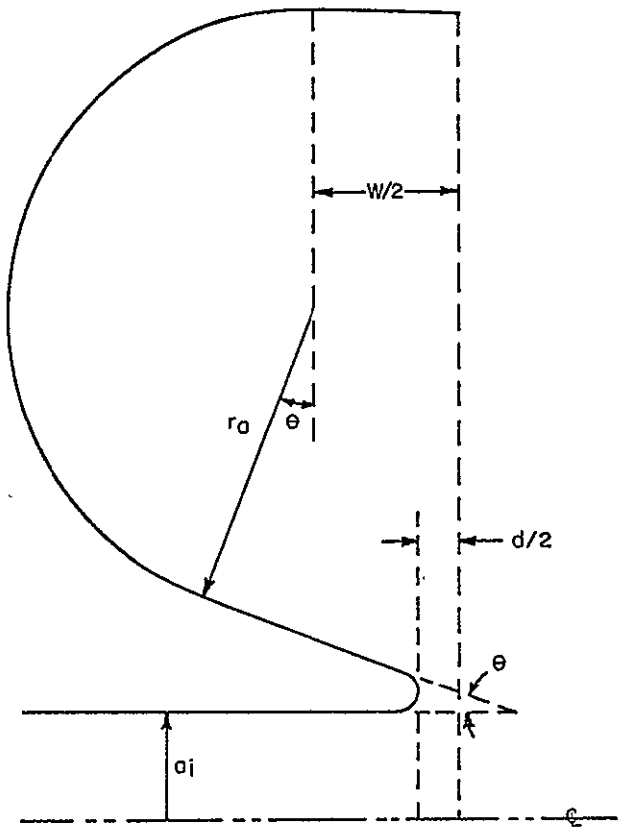

Figure 4 - Dimensions Required for Specifying Toroidal Cavity Boundary and Tunnel-Tip Radius of Curvature.

gap length of 0.020 inch correspond to a γa value of 1.05 and a 0.71 radian gap transit angle both of which lie near the values of 1 and 0.8 radian, respectively, indicated in the preliminary designs.

A cavity with round tunnel tips was analyzed in order to obtain a reference value which would show the anticipated improvement with such modifications as bevelling the tunnel tips, champfering the outer walls of the reentrant tunnel and rounding the cavity walls to form a toroidal shape (see Figure 5). An analysis of a series of three cavities with round tunnel tips and only the dimension marked ℓ varied, produced the results shown in Table VI. Data obtained from an analysis of three similar cavities having the tunnel tip tapered with a 20-degree bevel are also given in Table VI. A sketch of the device is shown in Figure 6. In another series of three calculations, the bevel was extended to form a smooth conical outline as shown by the dashed line in Figure 6. Results for these cases as well as values interpolated at the designed resonance frequency of 12.2 GHz are listed in the table.

The conical tunnel yields a much higher value of Q than the straight cylindrical tunnel. The lower losses result in part from the decrease in RF current density at the larger diameter of the tunnel root.

The properties of several toroidal cavities were then computed in order to determine the variation of resonance frequency with cavity size for the gap length, tunnel diameter, tunnel tip radius of curvature, and cone angle fixed at 0.020, 0.060, 0.005 inch, and 20 percent, respectively. Figure 7 illustrates the computed variation of the axial component of the electric field at three radii in the interaction gap. The computed parameters for this series of toroidal cavities are given in Table VII. The independent parameters are the torus arc radius r_a and torus center spacing parameter was defined in Figure 4.

Using the interpolated values of r_a = 0.0988 inch that was expected to yield a resonance frequency of 12.2 GHz, the cavity parameters were again computed and the results are given in Table VIII. For comparison, a conventional doubly-reentrant cylindrical cavity with bevelled tunnel tips was designed for this frequency and its properties computed by the relaxation program with the results also shown in Table VIII. The skin depth to wavelength ratio was evaluated for copper at 150°C and with an assumed 20 percent reduction in conductivity due to surface roughness so that a realistic value of the cavity internal Q could be calculated for both cavity types. The toroidal cavity is seen to have a 20 percent lower impedance-bandwidth parameter R/Q, as might have been anticipated since its shape inherently

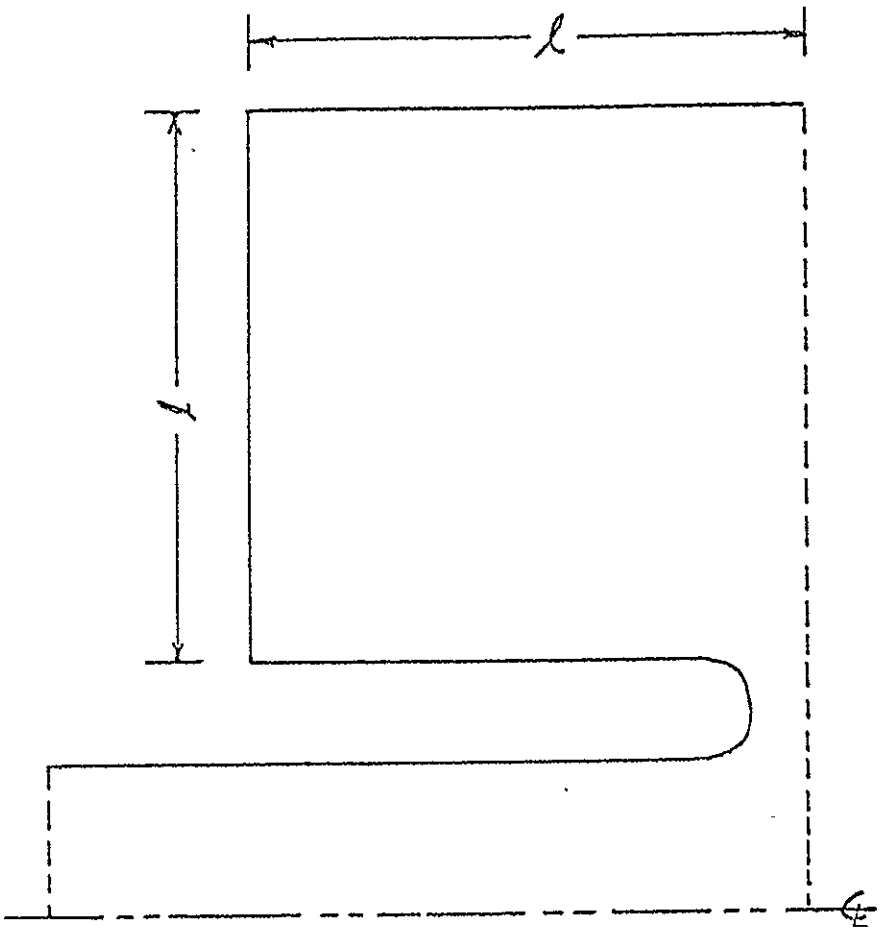

Figure 5 - Quadrant of Doubly-Reentrant Cavity with Rounded Tunnel Tips. (Tunnel I.D. 0.030 Inch, Tunnel O.D. 0.050 Inch and Interaction Gap 0.020 Inch)

TABLE VI - COMPUTED CAVITY PARAMETERS

Cavity Type	ℓ (inches)	O.D. (inches)	f_o (GHz)	R/Ω (ohms)	$\Omega\delta/\lambda$	Q_u
Round Tunnel Tips	0.11	0.32	12.68	69	0.0700	2820
" " "	0.13	0.36	10.80	74	0.0680	2970
" " "	0.15	0.40	9.52	86	0.0670	3110
" " "	(0.1136)*	(0.3272)	(12.2)	(70)	(0.0698)	(2870)
Beveled Tunnel Tips	0.11	0.32	13.38	100	0.0755	2960
" " "	0.13	0.36	11.45	110	0.0731	3100
" " "	0.15	0.40	10.05	114	0.0722	3270
" " "	(0.1205)*	(0.3405)	(12.2)	(106)	(0.0742)	(3050)
Conical Tunnels		0.32	14.09	91	0.0840	3210
" "		0.36	12.21	96	0.0840	3450
" "		0.40	10.85	92	0.0833	3630

*Interpolated values

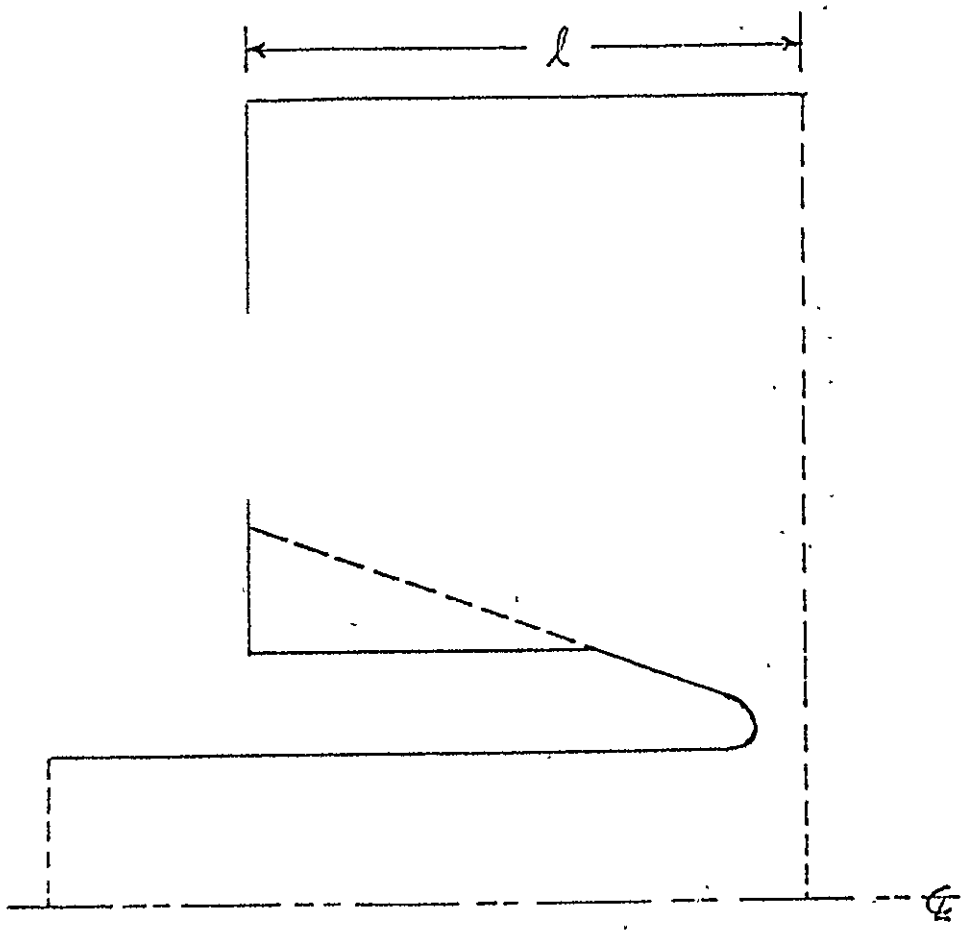

Figure 6 - Quadrant of Doubly-Reentrant Cavity with 20-Degree Tunnel-Tip Bevel. (In the Case of Doubly-Reentrant Cavities with Conical Tunnels, Beveled Surface Extends Back Toward End Wall as Indicated by Inclined Dashed Line)

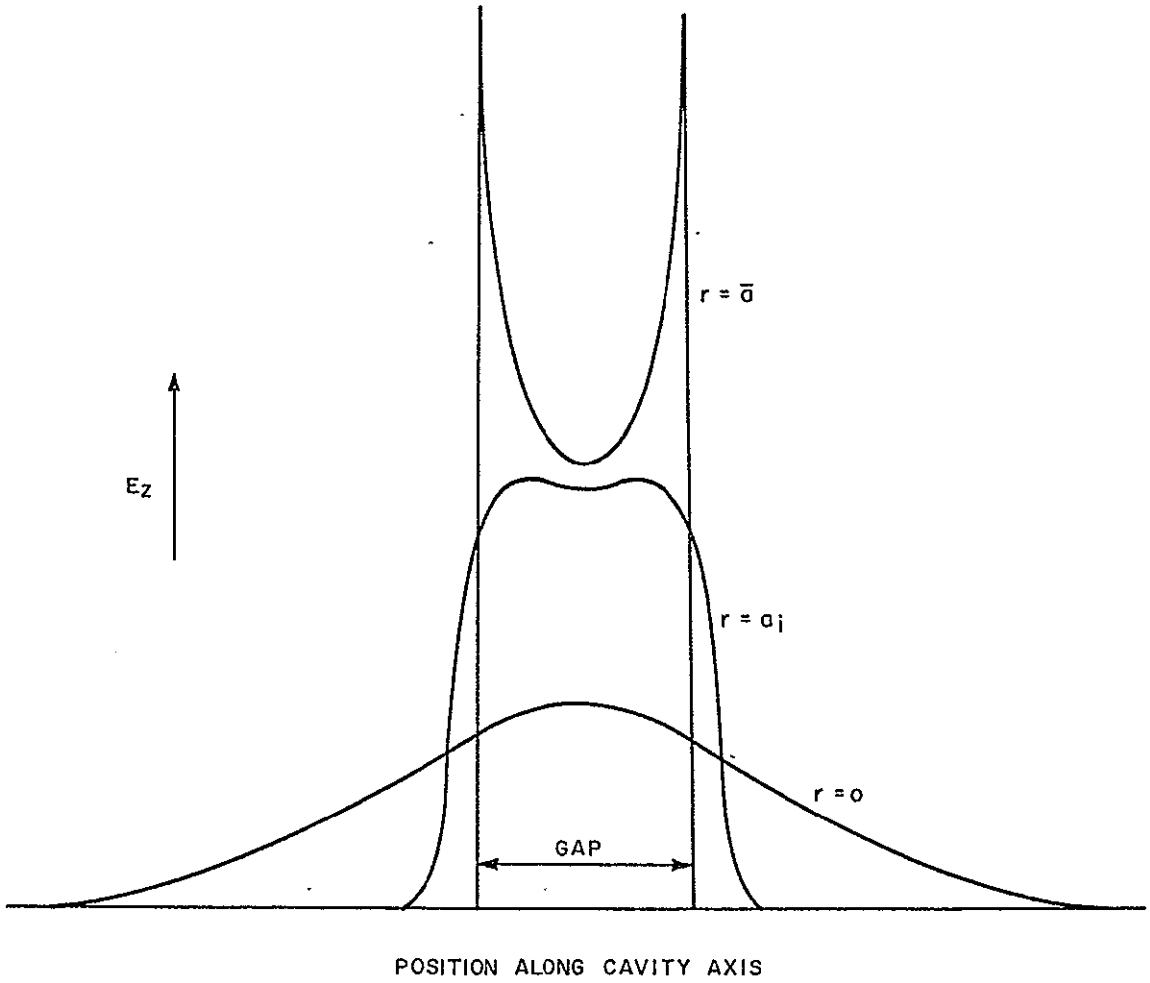

Figure 7 - Computed Variation of Axial Component of Electric Field at Three Radii in Interaction Gap of Toroidal Cavity. (Tunnel Radius is a_i and Radius at Tunnel Tip is $\bar{a}$)

TABLE VII - COMPUTED TOROIDAL CAVITY PARAMETERS

r_a (inch)	w (inch)	f_o (GHz)	R/Q (ohm)	$Q\,\delta/\lambda$
0.0785	0.0785	12.41	86	0.0880
0.0747	0.06	13.44	78	0.0999
0.0900	0.02	13.30	103	0.1010
0.0980	0.02	12.37	110	0.1040
0.1000	0.02	11.91	113	0.1040

- - - - - - -

TABLE VIII - COMPUTED CAVITY PARAMETERS AT 12.2 GHz

Cavity Type	Micro-perveance	R/Q (ohm)	$Q\,\delta/\lambda$	Q_i*	Cavity Width (inch)	Cavity O.D. (inch)
Toroidal	0.5	117	0.1084	2670	0.221	0.506
Toroidal	1.0	110	0.1042	2570	0.218	0.485
Conventional	1.0	137	0.0746	1840	0.245	0.345

*Computed for copper at 150°C with an assumed 20 percent reduction in conductivity due to surface roughness

- - - - - - -

introduces more shunt capacitance than the conventional cavity. The internal Q of the toroidal cavity is, however, 40 percent higher, which at the same bandwidth and gap impedance level results in a 20 percent reduction in internal power dissipation. Also shown in Table VIII are the toroidal cavity parameters computed for the narrowband 0.5 microperveance klystron.

THERMAL ANALYSIS OF CAVITIES

An essential part of the analytic design procedure for developing cavities for klystrons requiring high circuit efficiency is an analysis of the thermal characteristics of the reentrant portions of the cavity. Since cooling channels

are not feasible in the very thin tunnel walls required for the reentrant noses in cavities at a 12.2-GHz center-band frequency, the tunnel walls must be thick enough to keep the tunnel tip temperature well below the point where mechanical integrity is assured. Also, the lowest possible temperature must be maintained in order to reduce the surface resistivity of the copper. Increasing the thickness of the tunnel walls, however, adds shunt capacitance to the interaction gap with a consequent reduction in R/Q. This results in a higher value of loaded Q required to achieve a desired gap impedance, with consequent lower circuit efficiency. Accordingly, an approximate analytic solution was programmed for the computation of the thermal differences in a general biconical, hollow tunnel.

A reasonable assumption relative to cylindrical reentrant tunnel noses is that the isotherms are normal to the axis. Based on this simplifying assumption, the problem of heat flow in such tunnels reduces to a one-dimensional problem that can be solved by direct integration. The basic assumptions and boundary conditions are as follows:

(1) Isotherms in hollow tapered cylinders are normal to the axis.

(2) The main body of the cavity is maintained at a temperature of 150°C. (The optimum operating temperature of a water-filled heat pipe.)

(3) The thermal coefficient of resistivity for annealed copper at 12.2 GHz is the same as its measured DC value of 0.00393 per degree centigrade.

(4) The effective temperature of the tunnel in determining the tunnel surface resistivity is the mean temperature of the reentrant portion of the tunnel.

(5) Of the total beam power incident on the output gap reentrant tunnel, one half is concentrated on the tunnel tip and one half is distributed over the inner surface of the reentrant portions of the tunnel. (These fractions are an input parameter that may be varied.)

(6) One-third of the total RF power lost by thermal dissipation in the cavity walls is distributed uniformly in each reentrant tunnel and one third is lost in the remainder of the cavity walls.

A BASIC time-sharing computer program was written to compute the temperature rise at the tunnel tip and to derive the corresponding decrease in the unloaded Q of the cavity and the accompanying reduction in circuit efficiency. The program assumes that the entire tunnel can be represented

by two tandem hollow cylinders with conical outer surfaces as illustrated in Figure 8. The two sections in tandem with different cone angles are able to represent accurately: (a) a conventional standard cavity with a beveled tunnel tip or; (b) a toroidal cavity with an initial cone angle followed by a flaring section where the toroidal curve originates.

With the above assumptions, the temperature rise ΔT in one conical section is given by:

$$\Delta T = \int_o^{\ell} \frac{W_o \left(1 + \frac{W_1 x}{W_o \ell}\right)}{\pi \sigma_o \left[(r_1 + x \tan \theta)^2 - r_o^2\right]} \, dx \qquad (15)$$

Where:

x = distance measured from the tunnel tip

ℓ = length of conical section

θ = cone angle

W_o = beam power incident on the tunnel tip

W_1 = thermal power generated in the tunnel by RF losses and by beam incidence

σ_o = thermal conductivity of copper (assumed not to vary appreciably in the temperature range of 150 to 400°C)

r_o = tunnel inner radius

r_1 = outer radius at the tunnel tip

Since the RF losses are a function of tunnel temperature, the tunnel temperature must be computed by a reiterative process, with about five iterations required for convergence.

A time-sharing Fortran library program using the nodal method for solving heat conduction problems was employed to check the validity of the approximate analytic solution. The nodal program solves the required simultaneous equations for up to 42 nodes in a net-point representation of the heat conductor configuration.

A nodal diagram of a quadrant of a cylindrical doubly-reentrant cavity with conical noses is shown in Figure 9. Each nodal area is labelled with the temperature computed at its center. As indicated in the figure, the outer

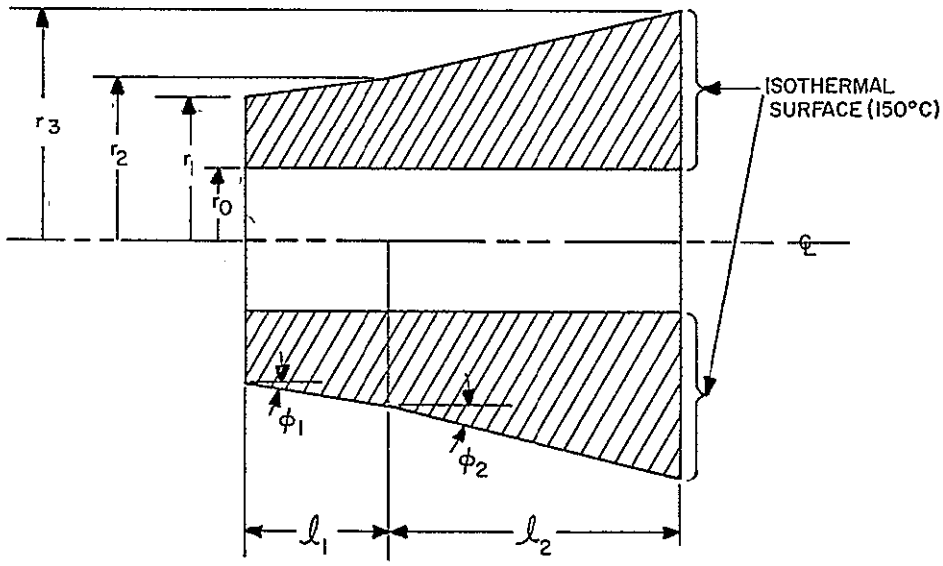

Figure 8 - Biconical Reentrant Cavity Tunnel

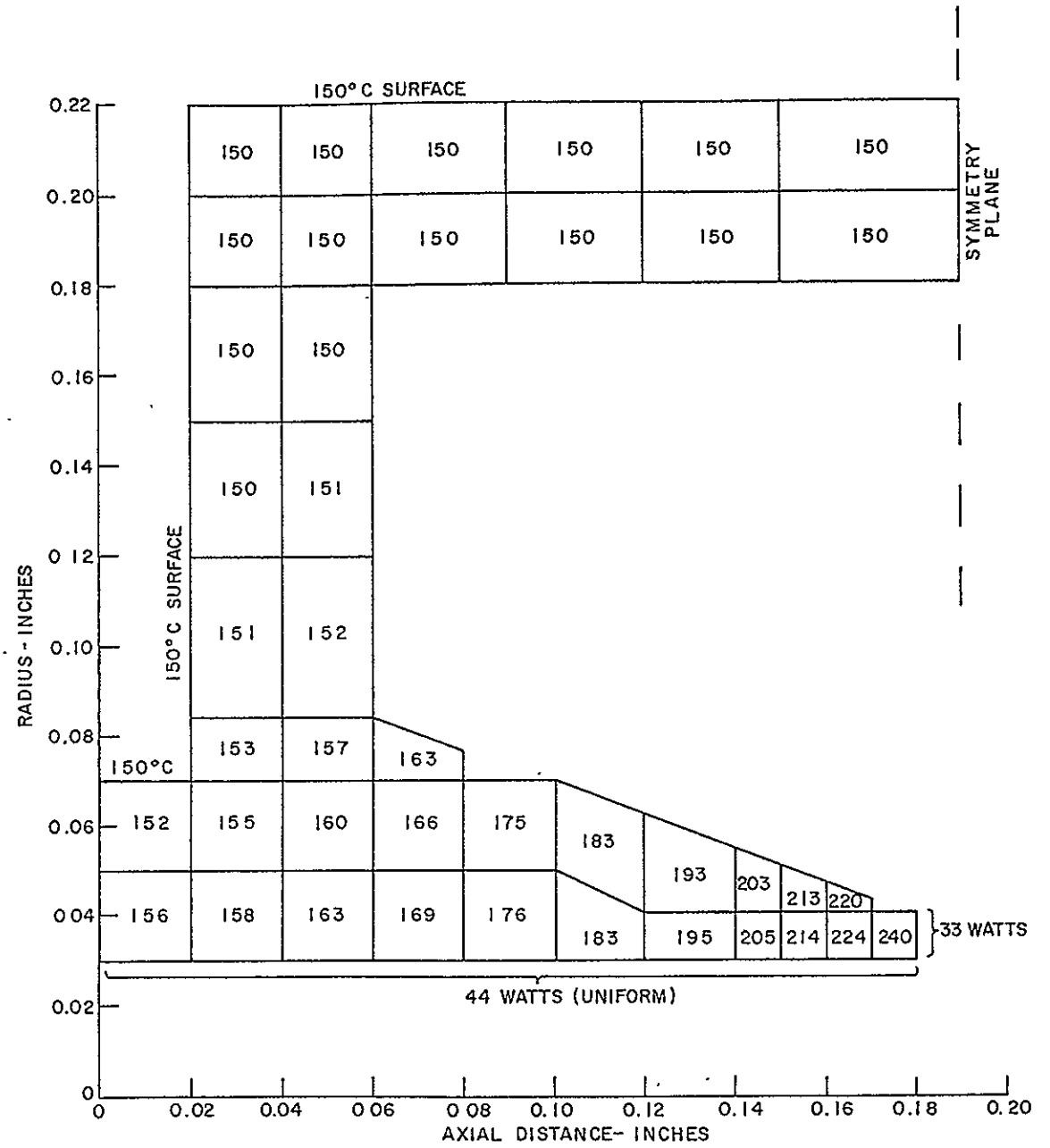

Figure 9 - Computed Thermal Distribution in Cylindrical Doubly-Reentrant Cavity

surface was maintained at a temperature of 150°C and a typical power input of 33 watts was assumed to be incident on the tunnel tip, with 44 watts being distributed uniformly on the tunnel wall. The computed equilibrium temperature in the node near the tunnel tip is 240°C and the temperature linearly extrapolated to the tunnel tip is 248°C.

The analytic solution is based on the simplifying assumption that the isotherms in the reentrant tunnel portion of the cavity are normal to the cavity axis. The validity of this assumption can be verified by an inspection of the temperature diagram in Figure 9, which shows that there is little variation in the computed temperature for nodes lying in vertical columns in the reentrant portion of the cavity.

On the basis of an average tunnel base temperature of 163°C as deduced from Figure 9, the temperature computed by the analytic program at the tunnel tip is 238°C, in reasonable agreement with the tip nodal temperature of 240°C and the extrapolated tip temperature of 248°C. It is concluded, therefore, that the analytic program, if used conservatively, is adequate for the analysis of the temperature rise in cavity tunnel tips.

THERMAL PROPERTIES OF OUTPUT CAVITIES FOR MICROPERVEANCE 0.5 and 1.0 KLYSTRONS

The toroidal cavity for the microperveance 1.0 klystron first considered has a relatively sharp tunnel tip with a cone angle of 20 degrees. The initial design made for the microperveance 0.5 klystron has a blunter tip with a cone angle of 30 degrees. As discussed below, the objective of the larger cone angle is to sacrifice a portion of the cavity R/Q for a lower operating temperature at the tunnel tip.

The thermal analysis for both a standard doubly-reentrant cavity and a toroidal cavity for the higher perveance klystron are given in Table IX. As stated above, the maximum allowable beam interception of 2 percent is assumed, with 0.5 percent distributed along the entire klystron body exclusive of the output cavity region, 0.5 percent incident on the exit tunnel tip and 0.5 percent on each of the interior surfaces of output gap tunnel. Also, there is an assumed Q degradation of 20 percent due to surface roughness at 12.2 GHz, which a later measurement has shown may be too conservative.

The comparison of the characteristics of a standard conventional cavity and a toroidal cavity given in Table IX shows that the parameter $Q\delta/\lambda$ in a toroidal cavity is over 40 percent higher than in a comparable

TABLE IX - COMPUTED OUTPUT CAVITY PARAMETERS FOR MICROPERVEANCE 1.0 KLYSTRON

Parameter	Cavity Type	
	Conventional	Toroidal
R/Q	137 ohm	110 ohm
$Q\,\delta/\lambda$	0.0750	0.1066
Cavity diameter	0.345 inch	0.493 inch
Cavity width	0.245 inch	0.221 inch
Q_u (at 150°C)	1840	2630
Operating temperatures		
Cavity walls	150 °C	150 °C
Adit tunnel tip	271 °C	188 °C
Exit tunnel tip	371 °C	247 °C
Q_u (at operating temperature)	1580	2510
Q_ℓ	79	83
Circuit efficiency (hot)	95.0 percent	96.7 percent
Tunnel diameter	0.060 inch	0.060 inch
Interaction gap length	0.020 inch	0.020 inch

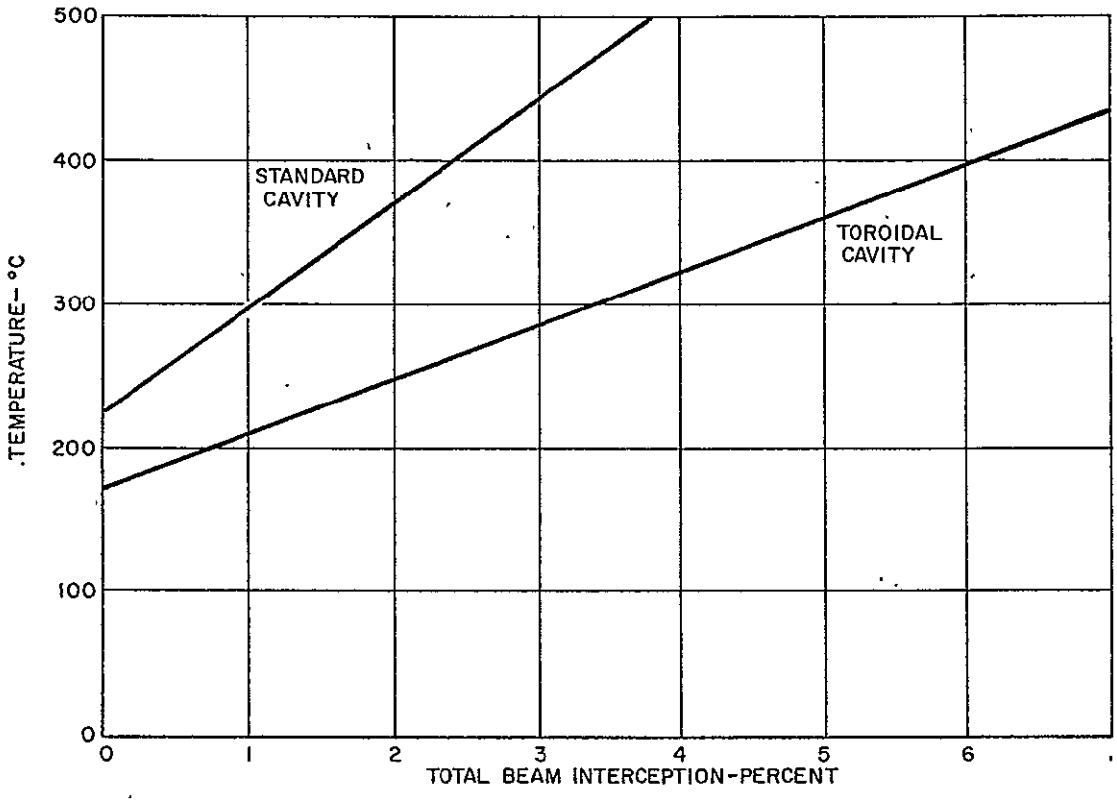

Figure 10 - Computed Variation of Exit Tunnel-Tip Temperature with Total Beam Interception in Perveance 1.0 Klystron

conventional cavity. Because of greater cooling capacity of the flaring toroidal tunnel, the temperature drop in the toroidal cavity is less than one-half that of the conventional cavity. Accordingly, at a beam interception of 2 percent, the internal-Q of the toroidal cavity is nearly 60 percent higher than that of the conventional cavity. The toroidal cavity as a result yields a circuit efficiency of 96.7 percent in comparison with the conventional doubly-reentrant cavity circuit efficiency of 95.0 percent under the same operating conditions.

The computed variation of the exit tunnel tip temperature as a function of total beam interception in the klystron is given in Figure 10. The corresponding variation of the circuit efficiency for the two cavity types as a function of beam interception is shown in Figure 11.

The computed results for a toroidal cavity for the lower perveance klystron are given in Table X. The assumed pattern of beam interception and the assumed Q degradation factor caused by surface roughness are the same as those for the cavities previously considered. Two modes of operation are under consideration. For the FM mode, the beam voltage is adjusted to 11.5 kV to yield approximately 4 kW of output power at saturation and for the AM mode the voltage is raised to 12.9 kV to yield approximately 5 kW of output power at saturation. The lower perveance klystron is expected to have 58 percent of the bandwidth of the higher perveance klystron and a circuit efficiency of 94.4 percent in comparison with 96.7 percent for the higher perveance klystrons. These advantages are offset by the fact that the internal conversion efficiency will be higher for the lower perveance klystron and problems in beam formation and collimation will be much less severe at the lower perveance.

The initial design of the toroidal cavity for the microperveance 0.5 klystron specifies a tunnel-tip cone angle of 30 degrees rather than the 20 degrees of the earlier design of the microperveance 1.0 klystron because it was believed that a blunter tip would be required to maintain the tunnel-tip temperature at a value below 400°C, as needed for long-term mechanical integrity. The thermal analysis shows, however, that with a body temperature of 150°C, the tip will reach only 238°C at the maximum beam interception of 2 percent. Thus, a sharper tip yielding a higher value of R/Q, and hence a lower Q_ℓ value with higher circuit efficiency, is feasible. Additional bandwidth for even greater phase linearity over the required band would be a byproduct of achieving a higher value of R/Q.

The computed variation of the exit tunnel-tip temperature with total beam interception and the corresponding circuit efficiency for both the AM

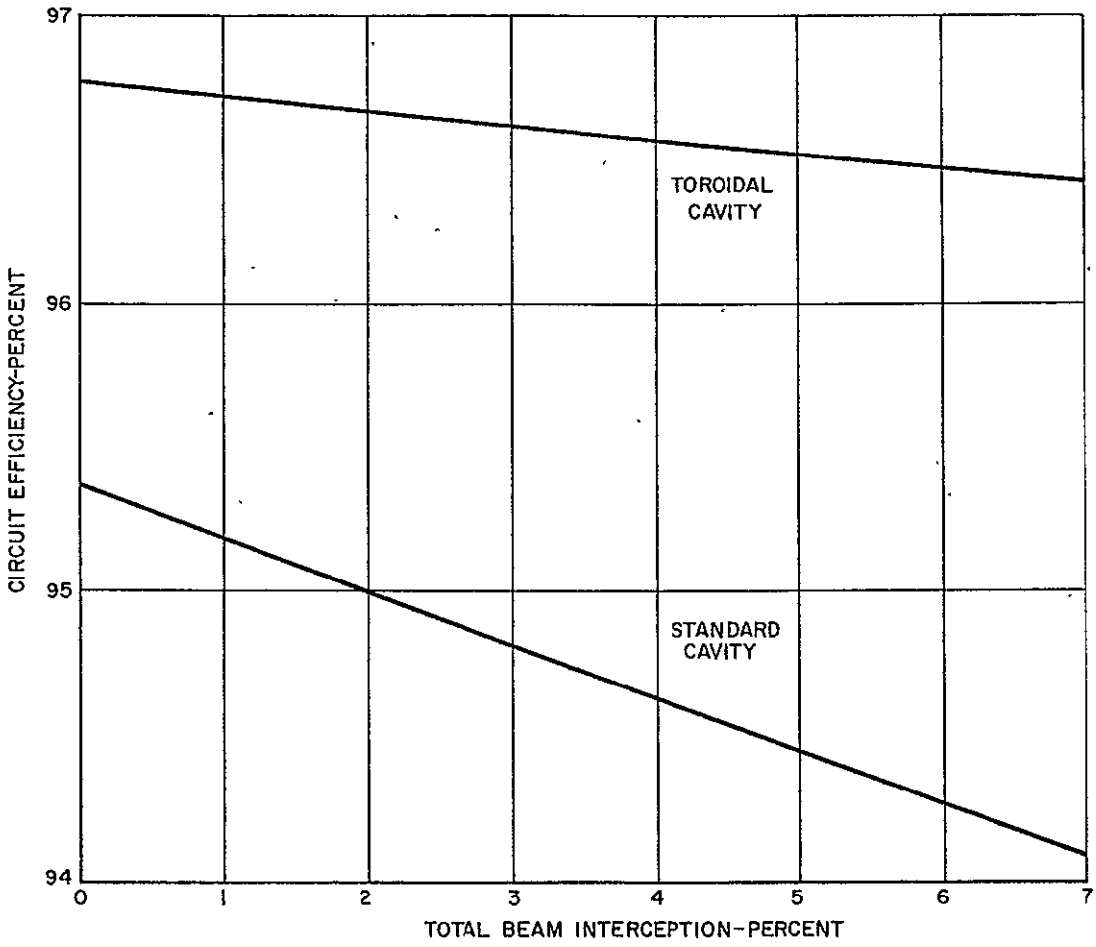

Figure 11 -- Computed Variation of Output Circuit Efficiency versus Beam Interception in Perveance 1.0 Klystron

TABLE X - COMPUTED OUTPUT CAVITY PARAMETERS FOR MICROPERVEANCE 0.5 KLYSTRON

Cavity Type	Toroidal	
R/Q	117 ohm	
$Q\,\delta/\lambda$	0.1084	
Cavity outer diameter	0.506 inch	
Cavity internal height	0.221 inch	
Tunnel inner diameter	0.066 inch	
Interaction gap length	0.024 inch	
Tunnel tip radius of curvature	0.005 inch	
Tunnel cone angle	30 °C	
Cavity Q_u (150°C)	2670	
Temperatures during saturation operation:		
	FM	AM
Cavity walls	150 °C	150 °C
Adit tunnel tip	190 °C	202 °C
Exit tunnel tip	238 °C	266 °C
Q_u at operating temperatures	2540	2510
Q_ℓ	143	143
Circuit efficiency	94.4 percent	94.3 percent

and FM modes of operation in the low-perveance klystron are shown in Figure 12. This cavity design exhibits very little degradation of circuit efficiency when the beam interception is increased from zero to a maximum of 2 percent. The curves can be used to estimate the loss in efficiency that would result if the cavity tip were redesigned to operate at a temperature of 400°C at the 2 percent beam interception level. In the FM mode, for example, Figure 12 shows that at a temperature of about 400 degrees the circuit efficiency is about 94.0 percent, a drop of 0.6 percent from its value at its anticipated operating temperature of 238 degrees. This loss may perhaps be offset by an increase in circuit efficiency afforded by the higher value of R/Q resulting from a sharper tip.

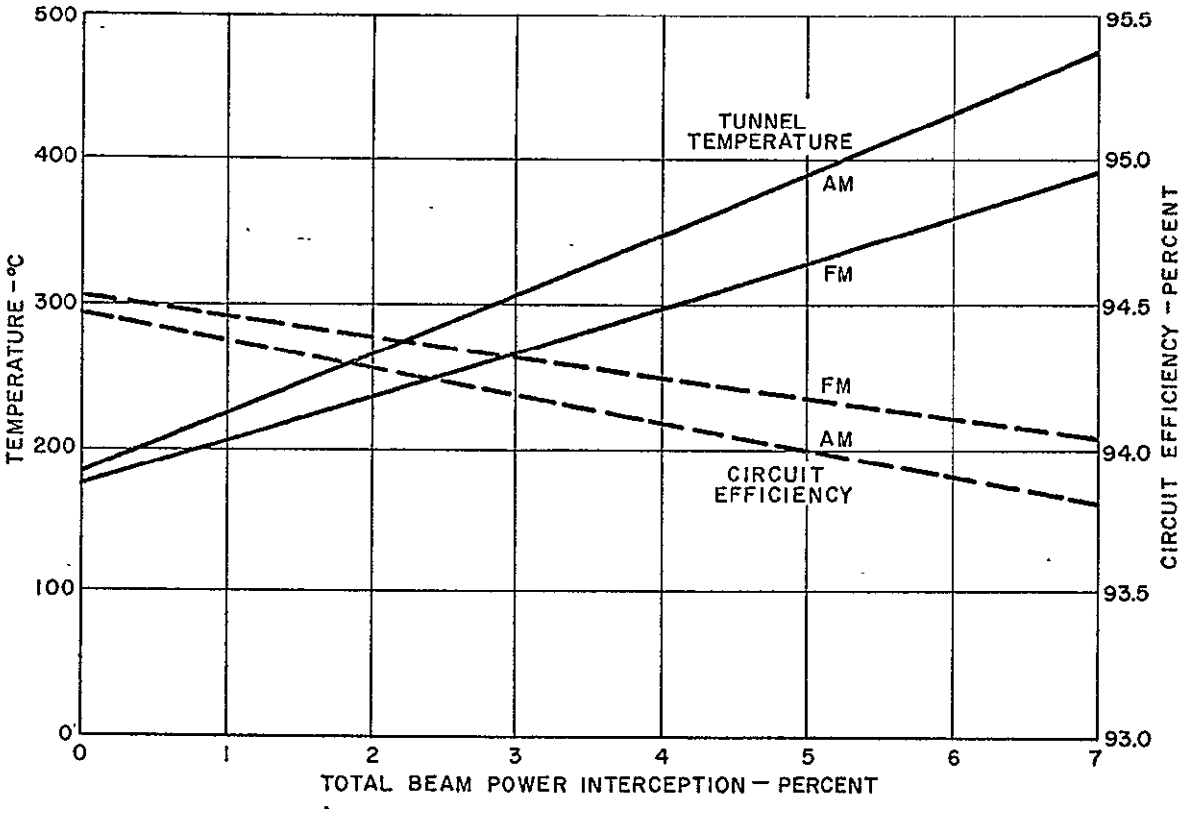

Figure 12 - Computed Variation of Exit Tunnel-Tip Temperature and Circuit Efficiency for Both AM and FM Operation in Perveance 0.5 Klystron

EXPERIMENTAL STUDY OF METHODS OF MINIMIZING LOSSES IN CAVITIES

OBJECTIVES AND GENERAL APPROACH

The objectives of the experimental aspects of the present study to enhance circuit efficiency are the following:

1) To investigate methods of cavity assembly, fabrication and joining to minimize internal power losses in klystron output cavities;

2) To demonstrate the mechanical feasibility of proposed new cavity designs as may be developed in the analytic study;

3) To investigate methods of cavity inner surface treatment that tend to reduce ohmic losses in the cavity;

4) To confirm by experimental measurement the basic parameters predicted for proposed new cavity types developed for the analytic study, and;

5) To measure the effect on internal Q of various output iris sizes and to develop loading curves as a function of iris dimensions.

Although the effect of various surface treatments on surface roughness and hence on the internal ohmic losses of cavities should be measured in cavities resonating at the specified frequency of 12.2 GHz, geometrical factors affecting cavity internal Q and the impedance-bandwidth parameter R/Q can most expeditiously be measured in cavities of larger size resonating at lower frequencies. Accordingly, the general experimental approach taken was to divorce the cavity configuration study from the direct measurement of the effect of surface treatment on surface resistivity. This was done by measuring the internal Q of right-circular cylindrical ("pill-box") cavities constructed in copper and resonating at a C-band frequency approximately one-half that of the desired 12.2 GHz final frequency. After surface treatment and machining techniques had been studied at 6 GHz, a series of half-size pill-box cavities resonating at 12 GHz were then constructed and tested to determine the variation of internal cavity Q at the higher frequency.

Because of the greater experimental accuracy at the lower frequency, the new toroidal cavities were constructed only at twice scale to resonate near 6 GHz. Methods of fabrication and assembly were used, however,

that could readily be used on half-size parts. After the development of experimental data on achievable copper surface resistivity at both 6 GHz and at 12 GHz, the measured results on toroidal cavities at 6 GHz can be reliably and confidently extrapolated to 12 GHz.

STUDIES WITH C-BAND DEMOUNTABLE CYLINDRICAL CAVITIES

The construction of a series of seven demountable cavities resonating near 6 GHz was undertaken for the study of the effect of surface treatment on RF cavity losses. The cylindrical shape was chosen because the exact geometrical cavity parameters R/Q and $Q\,\delta/\lambda$ are known and thus do not confuse the experimental results. The cavities are assembled from two halves joined at a midplane between the flat end faces; the joint thus being in a plane normal to the cylinder axis. When assembled, the cavities have a 0.5-inch internal height and an internal diameter of 1.5 inches and are constructed of copper. The mating surfaces of the two halves have a 1/2-degree bevel so that contact is made in a very thin rim on the inner wall of the cavity. Small holes are drilled in the end walls for the insertion of RF probes and dielectric perturbers; the walls are of sufficient thickness to make the apertures act as waveguides well below cutoff.

In Figure 13, the two halves of the cavity are shown adjacent to a six-inch scale. Also shown in the photograph are the stainless-steel plates, bolts, and retainer ring used for clamping the assembled cavity. The purpose of the retainer ring is to prevent lateral spreading of the soft copper cavity walls. The assembled cavity is shown in Figure 14.

The compression joint between the two halves of the copper cavity was found to give good RF contact, and the cavity could be taken apart and reassembled with reproducible results. When the cavity was first assembled, with only negligible manual tightening of the clamping bolts, a cavity internal Q of about 600 was measured by transmission methods. With moderate tightening of the bolts with a wrench, the cavity Q suddenly increased to approximately 7400 and remained at that value independent of additional clamping pressure. The theoretical Q for this cavity with ideally smooth copper walls is 8950.

The cavity shown in Figure 13 has a surface roughness ranging between 15 and 30 microinches as determined from profilometer measurements and by visual comparison with standard roughness gauges. (This range is comparable with the skin depth in copper at 6 GHz, which is computed to be 30 microinches.) The observed resonance frequency of 6024 MHz and the measured R/Q of 122 ohms agree well with the theoretical values of 6025 MHz and 123 ohms.

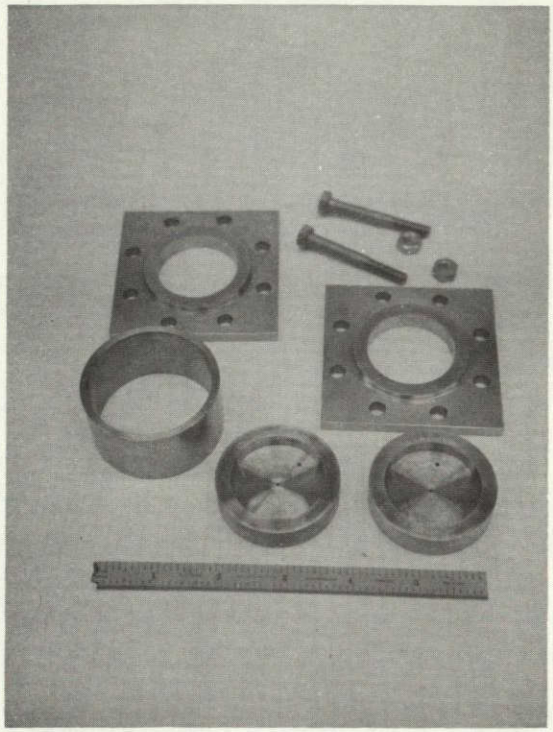

Figure 13 - Demountable C-Band Pill-Box Test Cavity Parts

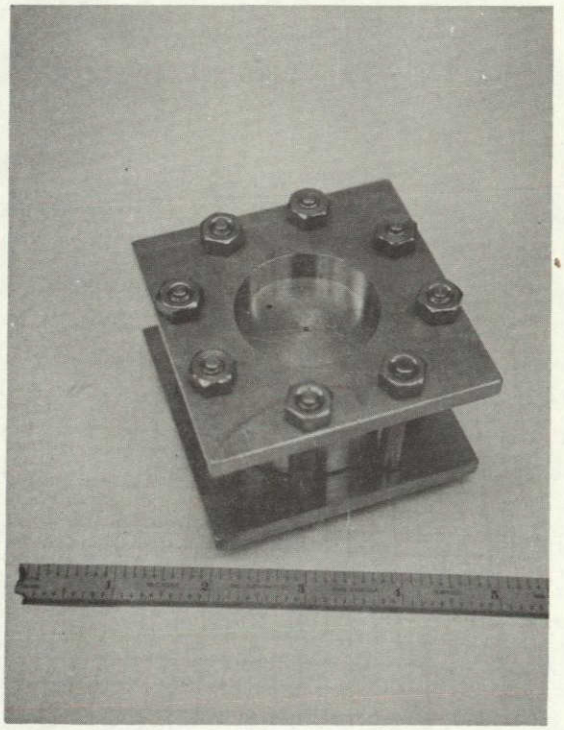

Figure 14 - Assembled C-Band Pill-Box Test Cavity

This cylindrical cavity was subsequently electropolished in a standard procedure described below and the Q improved to 8760.

Prior to the series of Q measurements, tests were made to determine whether or not the input and output coupling loops used in the transmission measurements were loading the cavity with a resulting decrease in the apparent cavity Q. The positions of the loops relative to the inner wall of the cavity are determined by a pair of micrometer gauges, and the apparent Q of the cavity is measured as a function of the distance that the tips of the loops are retracted into the cavity wall. It was observed that the loading of the loop becomes negligible when the loop is retracted at least 0.020 inch. Accurate measurements become increasingly difficult to make at retractions greater than 0.020 inch because of the greater attenuation of the transmitted power; however, reasonably reproducible results can be achieved at retractions between 0.020 and 0.030 inch.

The results of the Q measurements on the seven cavities are listed in Table XI. For each cavity at least 10 independent measurements of Q were made. Both the average value and the standard deviation are given.

- - - - - - -

TABLE XI - PROPERTIES OF CLAMPED DEMOUNTABLE PILL-BOX CAVITIES AT 6 GHz

No.	Surface Treatment	Surface Roughness	Theoretical Q	Measured Q
1	Electropolished	15-30 μ inch	9005	8760 ± 100
2	Lard-oil machined, oxidized in air at 650°C for 5 min., reduced in H_2	32 μ inch	8860	8450 ± 120
3	Lard-oil machined. Fired in H_2	16 μ inch	8820	8200 ± 80
4	"Machinist's best"	10 μ inch	8900	8520 ± 120
5	Rough-cut	150-200 μ inch	8820	7580 ± 80
6	Good machining (Grade 2-3)	16-20 μ inch	8920	8390 ± 210
7	Good finish with beveled corners	20-32 μ inch	8940	7280 ± 70

The first four pill-box cavities resonating at 6 GHz were subsequently used in a study of the effect of brazing and electron beam welding methods of joining the two halves. Cavity No. 1 was joined by electron beam welding and cavity Nos. 2, 3 and 4 were joined by standard Au-Cu foil brazing. The internal Q of each of the cavities was obtained from a series of measurements. The results of these measurements are given in Table XII.

- - - - - - -

TABLE XII - PILL-BOX CAVITY Q MEASUREMENTS AT 6 GHz

Cavity	State	Internal Q
1	As machined, clamped joint	7430
	Electropolished, clamped joint	8760 ± 100
	Electropolished, beam welded joint	9160 ± 350
	Electropolished, after two weeks exposure to air	8830 ± 120
	Electropolished, after H_2 firing	8540 ± 170
	Theoretical value	9005
2	As machined, clamped joint	7970 ± 80
	After oxidation and reduction, clamped joint	8450 ± 120
	Electropolished, clamped joint	8790 ± 90
	Electropolished, 0.0008 inch Au-Cu Eutectic (65-35) Alloy foil brazed joint	8700 ± 200
	Theoretical Q before brazing	8860
	Theoretical Q after brazing	8800
3	As machined, clamped joint	7600
	After H_2 firing, clamped joint	8200 ± 80
	Electropolished, clamped joint	8780 ± 125
	Electropolished, 0.002 inch Au-Cu Eutectic (65-35) Alloy foil brazed joint	8850 ± 160
	Theoretical Q before brazing	8820
	Theoretical Q after brazing	8770
4	As machined, clamped joint	7670 ± 150
	Electropolished, clamped joint	8710 ± 110
	Electropolished, 0.001 inch Au-Cu (50-50) Alloy foil brazed joint	8721 ± 90
	Theoretical Q before brazing	8900
	Theoretical Q after brazing	8880

Although the beam welding caused no significant change in the pill-box cavity height, it was discovered that the brazed cavities suffered a reduction of 0.001 to 0.005 inch in internal height. The reduced height affects the theoretical value of Q_i, hence Table XII shows a theoretical value of Q_i for assumed perfectly smooth surfaces both before and after brazing. The results given in Table XII demonstrate that both electron-beam welding and brazing with Au-Cu eutectic alloy yield good low-loss joints. Electron beam welding appears to provide greater dimensional stability, although it is quite possible that the subsequent high-temperature firing required in the final processing of the klystron would produce the same eventual distortion in a cavity even with beam-welded joints.

A phenomenon not fully evaluated but nevertheless making electron beam welding appear less attractive is that after two weeks of exposure to air at normal room temperature and humidity conditions, a marked deterioration in the measured value of the beam-welded cavity Q_i was noted. As shown in the table, firing in H_2 at 900°C for approximately three minutes failed to restore the cavity to its original high-Q state.

In order to measure directly the effect of surface treatment on surface resistivity at 12 GHz, a series of four pill-box cavities was constructed with a 0.747-inch diameter and an internal height of approximately 0.263 inch. The dimensions and measured internal Q of the four cavities and the resonance frequency both before electropolishing and after electropolishing are tabulated in Table XIII. As a comparison, the average value of Q_i after electropolishing was 6050 ± 90, while the computed theoretical value (with ideally smooth copper surfaces) was 6560. Thus at 12 GHz the value of the surface resistivity of the electropolished surface is increased by a factor of 1.084 over that of an ideally smooth surface. At 6 GHz, however, the surface resistivity of electropolished machined copper was found to have increased on the average, by a factor of 1.016.

- - - - - - -

TABLE XIII - MEASUREMENT OF PILL-BOX INTERNAL Q AT 12 GHz

Cavity No.	Q_i (as machined)	Q_i (electropolished)	h (inch)	Diam. (inch)	Resonance Freq. (GHz) (before)	(after)
K1	4810 ± 80	6110 ± 100	0.265	0.748	12.034	12.017
K2	4940 ± 100	6110 ± 70	0.262	0.747	12.032	12.020
K3	4860 ± 90	5980 ± 140	0.263	0.747	12.018	12.000
K4	4960 ± 50	6010 ± 70	0.263	0.747	12.021	12.006

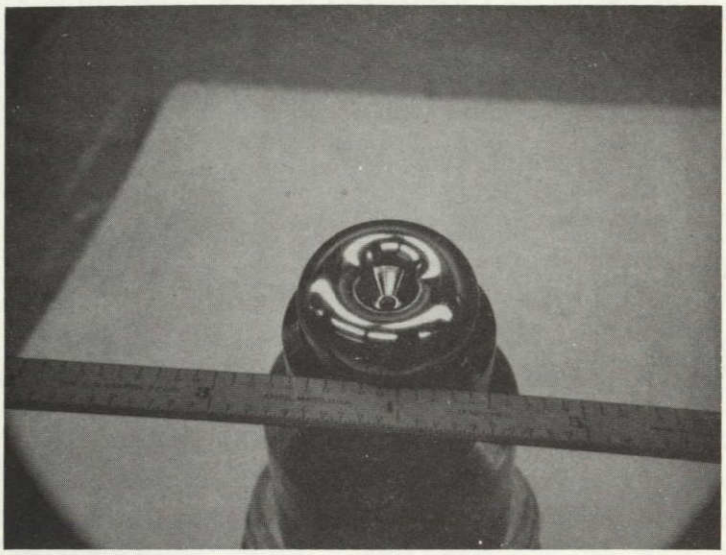

Figure 15 - Hardened Polished Steel Die Used to Coin Copper Toroidal Cavity Halves

FABRICATION OF TOROIDAL CAVITIES BY COINING

Coining or die-forming was deemed the most feasible method for fabricating toroidal cavities at 12 GHz. A steel die, illustrated in Figure 15, was polished to a bright finish, subsequently hardened and pushed into annealed OHFC copper blanks by a hydraulic press. The smooth and bright surfaces produced resemble those of a newly-minted penny. The coining operation is performed in three or four successive steps with the copper being reannealed before each pressing operation.

With the die-forming process cavity halves are fabricated in which the reentrant tunnel is a solid conical post. Later, the tunnel is drilled, the tunnel tips properly shaped on a lathe, and the two halves are brazed or clamped together to form the completed toroidal cavity. All critical interior surfaces on which high current densities occur are formed by the smooth die. The only machined surfaces are at the tunnel tip and the interior of the tunnels where the RF currents rapidly reduce to zero.

MEASURED PROPERTIES OF COINED TOROIDAL CAVITIES

EXPERIMENTAL OBSERVATIONS

Of the six toroidal cavities fabricated by coining copper halves, the last cavity was rejected because of an accidentally damaged tunnel tip. Each of the five remaining cavities was assembled by clamping in the steel fixture similar to that shown in Figure 13. The resonance frequency, impedance-bandwidth parameter R/Q and the internal Q were determined from transmission measurements.

A dielectric rod perturbation technique was used for the measurement of R/Q. In each of the cavities a 0.024-inch diameter quartz rod placed on the axis of the interaction gap, caused a shift of approximately 16 MHz in the resonance frequency. The rod was of sufficient length to extend into each tunnel beyond the limit of detectable fringing fields. The formula for deducing R/Q from an observed frequency shift Δf from an initial resonance frequency f is the following:

$$R/Q = 1.144 \cdot 10^{10} \, \Delta f \, d_{eff} / \left[(k-1) b^2 f^2 \right], \text{ (MKS units)} \qquad (16)$$

where b is the radius of the dielectric rod of relative dielectric constant k and d_{eff} is an effective interaction gap length. The effective gap length for perturbation measurements depends on the fringing field distribution and can be accurately computed from either theoretical or experimental field distributions from the following definition:

$$d_{eff} = \left[\int_{gap} E_z(a, z) \, dz \right]^2 / \int_{gap} E_z^2(b, z) \, dz \qquad (17)$$

where a is the tunnel radius and b the dielectric rod radius. The two integrals are computed over an interval extending into the tunnels until the fringing fields reduce essentially to zero. In a gridded gap with no fringing fields into the beam tunnels, the effective length d_{eff} becomes the actual interaction gap length d. As computed from the field distribution obtained from the relaxation solution of the cavity fields, the ratio of d_{eff} to the length d in the toroidal cavities is 3.226.

The measured properties of the five toroidal cavities are given in the following table:

TABLE XIV - MEASURED PROPERTIES OF COINED TOROIDAL CAVITIES

Cavity No.	f_o (MHz)	R/Q (ohms)	Q_i
1	5670	88.4	5520 ± 75
2	5554	86.1	5680 ± 130
3	5754	83.8	6010 ± 65
4	5730	85.4	5780 ± 120
5	5749	84.9	5710 ± 90

- - - - - - -

Cavity No. 1 was subsequently disassembled and its two halves were electropolished. Upon reassembly, the resonance frequency of 5670 MHz was found to be essentially unchanged and the internal Q had increased to 5770 ± 140, a 4.5 percent improvement.

As shown in Table XIV the resonance frequencies of the first two cavities constructed are somewhat lower than those of the last three. The close agreement in frequency among the last three cavities is attributed to more uniform and accurate die-forming, which is the result of improved skill developed from experience. Accordingly, the average of the experimental results for cavity Nos. 3, 4 and 5 are assumed to definitive.

COMPARISON OF EXPERIMENTAL AND COMPUTED PROPERTIES OF TOROIDAL CAVITIES

It was experimentally observed that a slight deformation of the cavities caused by the clamping process reduced the interaction gap from its nominal value of 0.0498 inch to 0.0474 inch. Consequently, in order to make a direct comparison between analytic results and experimental observations, it was necessary to re-analyze the toroidal cavity by employing the actual dimensions. A new relaxation calculation was made and a comparison of the results with the measured parameters averaged for cavity Nos. 3, 4 and 5 are listed in the following table:

TABLE XV - MEASURED AND COMPUTED VALUES OF TOROIDAL CAVITY PARAMETERS

Parameter	Unit	Computed	Measured
f_o	MHz	5774	5744
R/Q	ohms	87.8	84.7
Q_i		6200	6090

- - - - - - -

The close correlation between the computed and experimental values of the resonance frequency and R/Q demonstrates that the reliable predictions of the relaxation computer program for cavity properties can be dependably used in the development of new cavity designs. The computed value of Q_i given in the table corresponds to the assumption of a perfectly smooth copper surface at 20°C. As demonstrated in the case of Cavity No. 1, the measured value listed in the table reflects the increase of 4.5 percent for expected improvement resulting from electropolishing the coined surfaces. It is anticipated therefore, that the conductivity of an electropolished coined copper surface will be within 4 percent of that of an ideally smooth copper surface at 6 GHz.

For electropolished coined cavities at 12 GHz, the expected value of Q_i is the measured value at 6 GHz divided by the square root of the frequency ratio and divided by the ratio 1.084/1.016. (The latter ratio is the observed increase in surface resistivity at 12 GHz due to decreased efficiency of electropolishing at the higher frequency.) Consequently, the expected value of Q_i at 12 GHz is 3920.

IRIS COUPLING BETWEEN TOROIDAL CAVITIES AND WAVEGUIDE

SELECTION OF WAVEGUIDE DIMENSIONS

In order to optimize the overall circuit efficiency in the output circuit between the amplifier klystron output cavity and the antenna, the output waveguide should be as large as possible with the limit being set at which the TE_{20} mode begins to propagate at the operating frequency of 12.2 GHz. An excellent choice would be a standard WR-90 X-band waveguide that has internal dimensions of 0.900 x 0.400 inches and a cut-on frequency of the TE_{20} mode at 13.11 GHz.

The standard waveguide at approximately twice the size of the WR-90 guide was needed for coupling to the low frequency developmental cavities. WR-187 rectangular guide with internal dimensions of 1.872 x 0.872 inches provides a scaling factor of 2.08. At this scaling factor a toroidal cavity designed for 12.2 GHz would resonate at 5.87 GHz (a convenient and well-instrumented frequency). Coupling methods and waveguide transitions developed at the lower frequency in WR-187 waveguide can then be readily scaled by the inverse factor to provide the coupling design at 12.2 GHz. The completed cavities were observed to resonate at 5.74 GHz instead of the planned 5.87 GHz, but this is sufficiently close so that iris dimensions for the final 12.2-GHz cavity coupled to WR-90 waveguide can be extrapolated from the low-frequency design data.

The transition between the cavity and the output guide is located at the midplane of the cavity, as sketched in Figure 1. The transition consists of a quarter-wave section of reduced-height WR-187 waveguide located between a 0.125-inch high section adjoining the cavity iris and the full-height (0.872-inch) output guide. The intermediate section is 0.572-inch high and 0.595-inch long. The end that adjoins the cavity has a curved surface which mates with the cylindrical outer wall of the toroidal cavity. In the vicinity of the iris, the radius of the right-circular cylindrical outer wall of the cavity is reduced to 0.5562 inch. This dimension is 0.030 inch greater than the cavity inner radius, thus making the iris wall 0.030-inch thick. The length of the lowest-height section adjacent to the cavity, measured from the middle of the iris outer wall to the first step is 0.366 inch.

A sketch of the waveguide transition (as scaled for WR-90 waveguide for coupling to the 12.2-GHz toroidal cavity) is given in Figure 16.

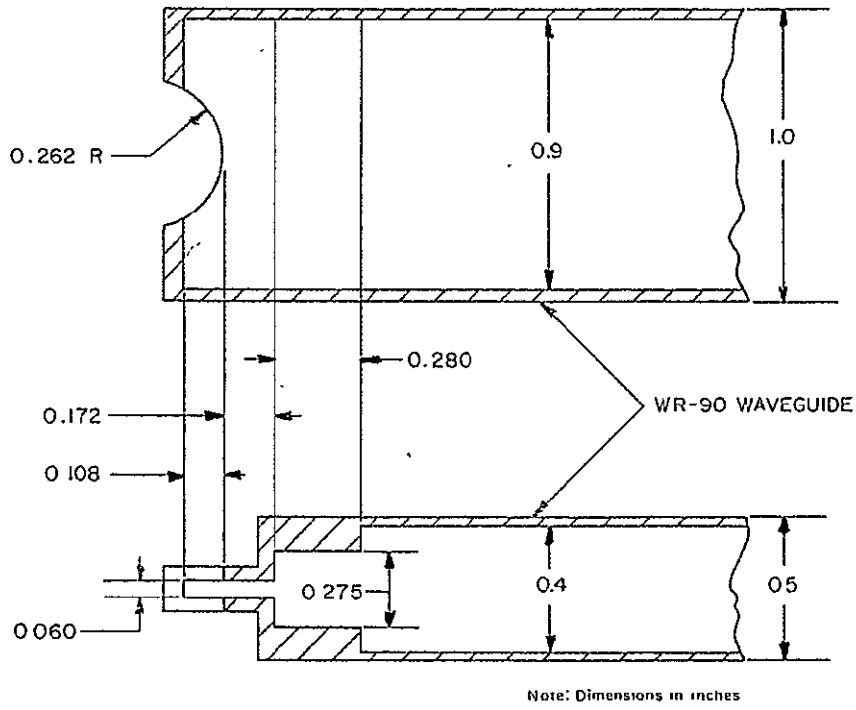

Figure 16 - Transition Between Cavity Iris and Output Waveguide

VARIATION OF COUPLING WITH IRIS SIZE

Cavity Nos. 3, 4, and 5 has slots 0.030, 0.040 and 0.050-inches high, respectively, which were located symmetrically at the cavity mid-plane. Initially, the slots were made 0.040-inch wide and in subsequent modifications, the width of the slots was increased to 0.45, 0.50, and 0.55 inches successively, to obtain additional coupling measurements. At each width, the cavities were clamped in the waveguide transition section; both the internal Q and the loaded Q were measured by the standard technique of measuring input VSWR and transmission of a signal through the cavity. This was done by means of a detector probe placed in the cavity tunnel and a signal generator connected to the output waveguide. From the standing wave ratio at the observed VSWR minimum as a function of frequency, the correction for series resistance in the transmission line and transition section were made.[8]

From the measured Q_i and Q_ℓ, the Q directly depending on iris size, Q_{ext}, was computed according to equation (2) with the results as tabulated in Table XVI. The values of Q_{ext} are also plotted as a function of iris dimensions shown in Figure 17.

- - - - - - -

TABLE XVI - MEASURED INTERNAL AND EXTERNAL Q's IN C-BAND CAVITIES WITH IRISES

Iris Width (inch)	Iris Height (inch)	Q_i	Q_{ext}
0.400	0.030	4090	2370
0.400	0.040	4560	1310
0.400	0.050	5560	1120
0.450	0.030	4400	732
0.450	0.040	4290	538
0.450	0.050	4140	426
0.500	0.030	3600	334
0.500	0.040	2790	215
0.500	0.050	2330	216
0.550	0.030	2370	147
0.550	0.040	2580	115
0.550	0.050	3470	108

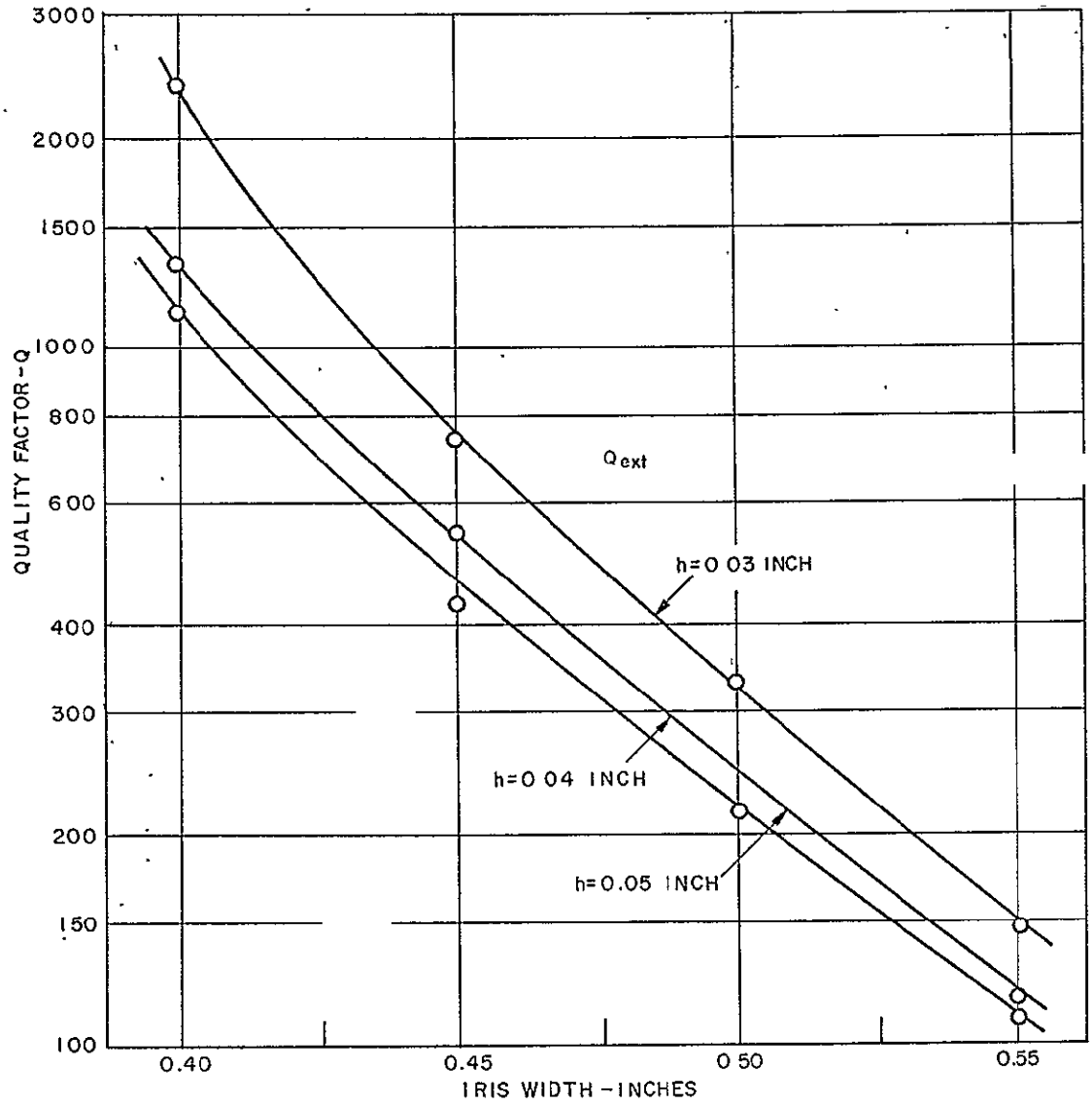

Figure 17 - Measured Variation of Q_{ext} With Iris Width and Height

The erratic variation of Q_i (listed in the third column of Table XVI) is evidence that the clamping technique is ineffective when the mating periphery of the two copper cavity halves is broken by a milled slot. Consequently, the results are indefinitive with respect to the dependence of internal Q on iris height or width. The Q_{ext} values are meaningful, however, despite the Q_i fluctuations because the Q_i contribution is subtracted from the Q_ℓ sum when Q_{ext} is computed by the reciprocal relationship of equation (2).

In order to obtain a more reliable measurement of the internal Q of an electropolished toroidal cavity with a coupling iris, cavity Nos. 3, 4 and 5 were disassembled, re-electropolished and reassembled by brazing. The mating edges of the copper halves were painted with a thin film of gallium and brazed in an evacuated bell jar at a temperature of 600°C. After brazing, cavity Nos. 3 and 4 were then individually soldered with a low-temperature tin-indium solder to the brass waveguide transition section. Soldering was not used to join cavity No. 5 to the waveguide transition since a satisfactory low-loss joint was obtained by clamping, with the solder foil shim functioning as a gasket between the cavity and the waveguide transition.

Each of the three cavity-waveguide transition assemblies was then connected to an X-band slotted waveguide for VSWR measurements. From the observed variation of VSWR with frequency the results listed in Table XVII were obtained. The measured values of the internal Q's of cavity Nos. 3, 4 and 5 were 5080, 4190 and 5040, respectively. In each case the measured value should be considered as a lower limit to the available Q_i in a toroidal cavity at this frequency range. The relatively low value of Q_i observed for cavity No. 4 is probably the result of an imperfectly brazed joint or of accidental contamination of the inner cavity wall with an excessive amount of gallium which was used to braze the joint. (The small tunnel size prevents a direct examination of the inner surface of the cavity and the cavity has not been sectioned for a microscopic examination of the brazed joint.) It is concluded that the values of 5080 and 5040 are more representative of the achievable values of Q_i in electropolished, brazed toroidal cavities at 5.7 GHz.

Since the resistivity of copper is proportional to the square root of frequency, the internal Q of a 12.2 GHz toroidal cavity with an iris of the relative dimensions of cavity Nos. 3, 4 or 5 would be about 3460 if electropolishing at 12.2 GHz were fully as effective as at 5.7 GHz. As discussed on page 47, electropolishing at 12.2 GHz was observed to be less effective than at 5.7 GHz by the ratio 1.016/1.084 or 0.937. Hence, the expected value of the internal Q at 12.2 GHz in a toroidal electropolished cavity with iris is 0.937 x 3460, or 3240.

TABLE XVII - MEASURED Q's OF BRAZED TOROIDAL CAVITIES

Cavity No.	Resonance (MHz)	$VSWR_{max}$	$VSWR_o$	$VSWR_{0.5}$	(MHz)	Q_ℓ	Q_i	Q_{ext}
3	5654	126	27	44	31	182	5080	189
4	5617	210	31	54	43	131	4190	135
5	5668	212	41	70	47	120	5040	123

- - - - - - -

RECOMMENDATION FOR COUPLING WITH MINIMUM INTERNAL POWER DISSIPATION

The frequency ratio 0.4708 is the scaling factor by which the C-band cavity resonating at 5744 MHz must be multiplied to produce cavity dimensions for resonance at 12.2 GHz. The R/Q will not vary from the value measured at C-band and will therefore be about 85 ohms at 12.2 GHz. The klystron design specified in Table III has a beam impedance of 19,000 ohms and a 0.7-radian gap transit angle which, according to the large-signal disk model simulations of the klystron, requires a gap impedance of approximately 17,000 ohms for maximum internal conversion efficiency in the output interaction circuit. Thus, the required value of Q_ℓ for maximum klystron efficiency is 200. The corresponding value of Q_{ext} required is in the vicinity of 215. As indicated in Figure 17, this value of Q_{ext} may be obtained with an iris 0.05 inch high and 0.5 inch wide, which dimensions scale to a height of 0.0235 inch and a width of 0.235 inch at 12.2 GHz. The thickness of the iris wall scales from 0.030 inch to 0.014 inch.

In a cavity with a negligibly small coupling iris, the internal Q at 12.2 GHz was deduced to be 3920 (refer to page 47). According to equation (3), the circuit efficiency for Q_ℓ and Q_i equal to 200 and 3920, respectively, is 94.9 percent. From the above extrapolation from a C-band cavity with an iris 10 percent larger than required for the desired coupling, the internal Q is 3240, corresponding to a circuit efficiency of 93.8 percent. By linear interpolation, therefore, the minimum value of circuit efficiency expected in the 12.2 GHz klystron is 93.9 percent.

In conclusion, the recommended output coupling system consists of 0.0235- by 0.235-inch rectangular iris that leads into a stepped-height

transitions section (dimensions shown in Figure 15). This transition section is coupled to the cavity standard WR-90 rectangular waveguide which in turn couples the klystron to the antenna. Excluding the small loss that would occur in the WR-90 waveguide between the transition and the antenna, the predicted circuit efficiency is approximately 94 percent.

RECOMMENDED TOROIDAL CAVITY DESIGN

DESIGN PARAMETERS

The proposed dimensions for a toroidal cavity to be used as the output circuit for a high-efficiency 4-kW satellite-borne television broadcast power amplifier at a center frequency of 12.2 GHz are tabulated in Table XVIII. Basic beam parameters matching the proposed cavity design are also tabulated. The recommended coupling iris and transition section between the cavity and standard WR-90 waveguide were described in the previous section.

RECOMMENDED FABRICATION PROCEDURES

It is recommended that the toroidal cavity be fabricated from symmetric halves formed by a coining process. A hardened polished steel die conforming in shape to the interior of the toroidal cavity -- excluding the reentrant tunnel openings -- may be used to form the cavity halves in annealed OFHC copper. The beam tunnels are then machined into the tunnel cones left by the die-forming process and the tunnel tips rounded to the specified radius of curvature. The precise shaping of the tunnel tip is extremely critical since slight variations will have a great effect on the cavity resonance frequency. Precision in shaping the curved walls of the cavity is a less difficult task because the machining is done on a convex steel surface which may later be hardened and polished. This is opposed to a concave soft copper surface which entraps foreign particles in the surface when it is mechanically polished.

When the die-forming and tunnel machining operations have been completed, the cavities should be cleaned by a conventional degreasing and bright-dipping procedure. Subsequently, the surfaces are electropolished with a DC etching current in a phosphoric acid electrolytic bath. The etching is performed only to a degree which is sufficient to remove surface defects without entailing an appreciable loss of copper from the entire surface. Following the etching process, the cavities should be washed in deionized water and alcohol and stored in a hot box until the final brazing. The recommended brazing method is gold foil, diffusion or indium diffusion brazing in a vacuum oven.

TABLE XVIII - HIGH-EFFICIENCY TOROIDAL OUTPUT CAVITY PARAMETERS AND SPECIFICATIONS

Resonance frequency		12.2 GHz
Nominal bandwidth		40 MHz
3-dB bandwidth		61 MHz
Circuit efficiency		94 percent
R/Q		85 ohms
Q_ℓ		200
Q_i		3240
Tunnel cone angle		30 degree
γ_a		1.0
Interaction gap transit angle		0.7
Beam voltage		11.0 kilovolts
Beam current		0.577 amperes
Beam perveance		0.5 microamperes/volt$^{1.5}$
Tunnel diameter	0.064 inch	0.163 cm
Internal diameter	0.4954 inch	1.258 cm
Interaction gap length	0.0223 inch	0.0567 cm
Tunnel tip radius of curv.	0.005 inch	0.0127 cm
Internal width of torus	0.2153 inch	0.5470 cm
Torus arc radius	0.0965 inch	0.2451 cm
Torus center spacing,	0.0233 inch	0.0567 cm
Coupling iris height	0.0235 inch	0.0600 cm
Coupling iris width	0.235 inch	0.600 cm
Iris wall thickness	0.014 inch	0.036 cm

DISCUSSION OF RESULTS

In this study, general design parameters were developed for a satellite-borne klystron for use in FM TV broadcasting at a four-kilowatt power level, and a frequency of 12.2 GHz. The specific requirements for the klystron amplifier output cavity were used in deriving an optimum cavity design with minimum internal power loss. Although an improved design was developed for this particular set of broadcast amplifier parameters, the results show that, in general, a toroidal cavity has lower internal losses than a conventional doubly-reentrant cavity with a pair of right-circular cylindrical reentrant tunnels.

Time limitations in the present study prevented a more thorough and systematic study of the effect of various parameter modifications on the physical description of the toroidal cavity. In particular, additional computations with the reentrant tunnel cone angle as an independent parameter would indicate the cone angle yielding the optimum value of R/Q and Q_i in a toroidal cavity. Although it is possible with the present analytic tools to develop a comprehensive set of design curves for toroidal cavities for klystrons at any power level or frequency, the scope of the present study could not encompass the more general analysis. It is recommended, however, that the present analytic methods be employed to develop these design curves which would be of general use.

The experimental study of the effect that coupling iris size has on the internal Q of the toroidal cavity agrees with the customary observation that the irises usually employed in conventional cavities reduce Q_i by approximately 10 percent. Lower limits for the internal Q of electropolished copper toroidal cavities coupled by means of rectangular irises to rectangular output waveguide were obtained by measuring the internal Q of three brazed copper cavities expediently joined by soft-soldering or clamping to a brass waveguide transition section. More definitive results could be obtained by further experimental studies involving a larger number of toroidal cavities fabricated in copper and brazed to copper waveguide transition sections to constitute permanently-bonded integral output circuits. Because of the possibility of variability in the contact ohmic losses, the presently observed value of internal Q leading to a circuit efficiency of 94 percent should be considered as a lower limit. The actual construction of a klystron employing a toroidal output circuit should be preceded by a specific design study in which the output coupling circuit is experimentally evaluated and improved.

CONCLUSIONS AND ACKNOWLEDGEMENTS

In an analytic and experimental study of methods of enhancing circuit efficiency in klystron power amplifiers for satellite-borne television broadcast service, a new type of toroidal cavity was developed. The toroidal cavity has a forty percent higher internal Q than an equivalent conventional doubly-reentrant cavity and under the same conditions of operation has 20 percent lower internal power dissipation. Fabrication methods developed during the study demonstrated the feasibility of cavity construction. The toroidal cavity was observed to exhibit the properties that were analytically predicted. A specific design for a 12.2 GHz, 4 kilowatt television transmitter was developed.

This work received substantial benefit from the direction, advice and consultation of its Project Manager at NASA, Mr. G. J. Chomos and from the continuing interest and advice of Dr. H. G. Kosmahl of NASA. The experimental aspects of this study were planned by Mr. R. A. Dehn, Manager of Tube Research, Microwave Tube Operation, General Electric Company, and the experimental work and study of fabrication methods was done by Mr. R. E. Turrentine of the Microwave Tube Operation.

REFERENCES

1. Branch, G. M., and Mihran, T. G., "Analytic Designs of a Space-Borne Magnetically-Focused Klystron Amplifier", NASA Document CR-72461, October 25, 1968

2. Ramo, S., Whinnery, J. R., and Van Duzer, T. R., "Fields and Waves in Communication Electronics", p. 252. John Wiley & Sons, New York; 1965

3. Branch, G. M., "Electron Beam Coupling in Interaction Gaps of Cylindrical Symmetry", Trans. IRE ED-8, pp. 193-207; May 1961

4. Branch, G. M., and Mihran, T.G., op. cit., pp. 22-30

5. Branch, G. M., and Mihran, T. C., op. cit., p. 32

6. Varian, R. H., and Varian, S. F., "A High Frequency Oscillator and Amplifier", JAP 10 pp. 321-327; May 1939

7. Chodorow, M., Ginzton, E. L., Jasberg, J., Lebacqz, J. F., and Shaw, H. J., "Development of High-Power Pulsed Klystrons for Practical Applications", Proc. IRE 47, pp. 20-29; January 1959

8. Malter, L., and Brewer, G. R., "Microwave Q Measurements in the Presence of Series Losses", JAP 20, pp. 918-925; October 1949

Appendix A
LISTING OF BASIC PROGRAM "TOROID"

```
TOROID    14:38   TUES    5-19-70

50 REM TIME-SHARING PROGRAM FOR CALCULATING TOROIDAL CAVITY
52 REM BOUNDARY COORDINATE PAIRS.
54 REM  WRITTEN BY G.M. BRANCH, MTO, SEPTEMBER 25, 1969.
56 REM INPUT TUNNEL RADIUS, TUNNEL TIP RADIUS, INTERACTION GAP
58 REM  LENGTH, LOCATION OF GAP MIDPLANE WITH RESPECT TO AN
60 REM  ARBITRARY Z AXIS ORIGIN, TUNNEL CONE ANGLE IN DEGREES,
62 REM DISPLACEMENT OF TOROIDAL CURVE CENTER OF CURVATURE FROM
64 REM GAP MIDPLANE (POSITIVE FOR DISPLACEMENT TOWARD ORIGIN),
66 REM RADIUS OF CURVATURE OF TOROIDAL CURVE.
68 REM
70 READ A1,B1,D1,P1,C3,W1,R1
72 LET C2=C3/57.2958
74 LET C1=COS(C2)
76 LET S1=SIN(C2)
78 LET T1=S1/C1
80 LET T2=T1*S1
82 PRINT "TABLE OF TOROIDAL CAVITY BOUNDARY PARAMETERS"
84 PRINT
86 PRINT "  W/2 =";W1,"   R =";R1
88 PRINT
90 PRINT "BOUNDARY POINT COORDINATES"
92 PRINT
94 PRINT "   X","   Y"
96 PRINT
98 PRINT 0,0
100 LET P2=P1-D1/2
102 PRINT 0,A1
104 LET X1=P2-B1
106 PRINT X1,A1
108 LET B2=B1/SQR(2)
110 LET R2=R1/SQR(2)
112 LET X1=X1+B2
114 LET Y1=A1+B1
116 PRINT X1,Y1-B2
118 PRINT P2,Y1
120 PRINT X1,Y1+B2
122 PRINT P2-(1-S1)*B1,Y1+C1*B1
124 LET Y2=A1+R1*T2+(W1-D1/2)*T1+B1*(1-T1+C1+T2)
126 LET X2=P1-W1
128 PRINT X2-R1*S1,Y2
130 LET Y2=Y2+R1*C1
132 PRINT X2-R2,Y2-R2
134 PRINT X2-R1,Y2
136 PRINT X2-R2,Y2+R2
138 LET Y2=Y2+R1
140 PRINT X2,Y2
142 PRINT P1,Y2
144 PRINT
146 PRINT "RADIUS OF CAVITY =";Y2
148 PRINT
150 GO TO 70
500 DATA .033,.005,.034,.12,30
501 DATA .012,.0985
999 END
```

Appendix B
LIST OF SYMBOLS

Symbol	Definition	Unit
a_i	Inner radius of cavity beam tunnel	inch, cm, m
c	Velocity of light	m/sec
d	Cavity interaction gap length	inch, cm, m
E	Electric field intensity	volt/m
H	Magnetic field excitation	amp/m^2
J_i	Ordinary Bessel function of ith order	---
k	Free space propagation constant ω/v	radian/sec
Q	Resonant circuit quality factor defined as the ratio of the stored to any specified energy loss per radian	---
Q_{ext}	External Q of cavity defined in terms of energy delivered per radian to external load	---
Q_i	Internal Q of cavity defined in terms of energy dissipated in ohmic losses internally	---
Q_ℓ	Loaded Q in terms of total energy delivered by cavity per radian	---
Q_u	Unloaded Q of cavity. Same as Q_i	---
R	Cavity interaction gap shunt resistance	ohm
r_a	Radius of toroidal arc	in, cm, m
r_i	Inner radius of cavity beam tunnel	in, cm, m
r_o	Outer radius of reentrant tunnel	in, cm, m

Symbol	Definition	Unit
R_s	Surface resistivity of metallic wall	ohm/square
U	Stored energy in a resonating cavity	joule
v	Velocity of wave propagation	m/sec
V	Interaction gap peak RF voltage	volt
W_o	Beam power	watt, kw
W_l	Ohmic power loss	watt, kw
β	Axial propagation constant ω/v	radian/m
γ	Radial propagation constant $\sqrt{\beta^2 - k^2}$	radian/m
δ	Skin depth in an imperfect conductor	in, cm, m
ΔT	Temperature increment	deg. C
ϵ	Permittivity of a dielectric medium	farad/m
ϵ_o	Permittivity of free space	farad/m
η	Intrinsic impedance of free space	ohm
η_{ckt}	Circuit efficiency	---
θ	Inclination angle of conical tunnel outer wall	radian, degree
λ	Wavelength	in, cm, m
λ_o	Free-space wavelength	in, cm, m
μ	Permeability of magnetic medium	hy/m
μ_o	Permeability of free space	hy/m
σ_o	Thermal conductivity	watt/(m deg. C)
ω	Angular frequency (2π x frequency)	radian/sec